Redox Biology 17 (2018) 70–88

Contents lists available at ScienceDirect

Redox Biology

journal homepage: www.elsevier.com/locate/redox

Identification of homocysteine-suppressive mitochondrial ETC complex genes and tissue expression profile – Novel hypothesis establishment

Ramon Cueto[a], Lixiao Zhang[a], Hui Min Shan[a], Xiao Huang[a], Xinyuan Li[a], Ya-feng Li[a], Jahaira Lopez[a], William Y. Yang[a], Muriel Lavallee[a], Catherine Yu[a,e], Yong Ji[f,*], Xiaofeng Yang[a,b,c,d], Hong Wang[a,b,c,d,**]

[a] Center for Metabolic Disease Research, Temple University - Lewis Katz School of Medicine, 3500 North Broad Street, Philadelphia, PA 19140, USA
[b] Department of Pharmacology, Temple University - Lewis Katz School of Medicine, Philadelphia, PA, USA
[c] Thrombosis Research Center, Temple University - Lewis Katz School of Medicine, Philadelphia, PA, USA
[d] Cardiovascular Research Center, Temple University - Lewis Katz School of Medicine, Philadelphia, PA, USA
[e] The Geisinger Commonwealth School of Medicine, Scranton, PA, USA
[f] Key Laboratory of Cardiovascular Disease and Molecular Intervention, Nanjing Medical University, Nanjing 210029, China

ARTICLE INFO

Keywords:
Database mining
Tissue expression profile
Homocysteine metabolism

ABSTRACT

Hyperhomocysteinemia (HHcy) is an independent risk factor for cardiovascular disease (CVD) which has been implicated in matochondrial (Mt) function impairment. In this study, we characterized Hcy metabolism in mouse tissues by using LC-ESI-MS/MS analysis, established tissue expression profiles for 84 nuclear-encoded Mt electron transport chain complex (nMt-ETC-Com) genes in 20 human and 19 mouse tissues by database mining, and modeled the effect of HHcy on Mt-ETC function. Hcy levels were high in mouse kidney/lung/spleen/liver (24–14 nmol/g tissue) but low in brain/heart (~5 nmol/g). S-adenosylhomocysteine (SAH) levels were high in the liver/kidney (59–33 nmol/g), moderate in lung/heart/brain (7–4 nmol/g) and low in spleen (1 nmol/g). S-adenosylmethionine (SAM) was comparable in all tissues (42–18 nmol/g). SAM/SAH ratio was as high as 25.6 in the spleen but much lower in the heart/lung/brain/kidney/liver (7–0.6). The nMt-ETC-Com genes were highly expressed in muscle/pituitary gland/heart/BM in humans and in lymph node/heart/pancreas/brain in mice. We identified 15 Hcy-suppressive nMt-ETC-Com genes whose mRNA levels were negatively correlated with tissue Hcy levels, including 11 complex-I, one complex-IV and two complex-V genes. Among the 11 Hcy-suppressive complex-I genes, 4 are complex-I core subunits. Based on the pattern of tissue expression of these genes, we classified tissues into three tiers (high/mid/low-Hcy responsive), and defined heart/eye/pancreas/brain/kidney/liver/testis/embryonic tissues as tier 1 (high-Hcy responsive) tissues in both human and mice. Furthermore, through extensive literature mining, we found that most of the Hcy-suppressive nMt-ETC-Com genes were suppressed in HHcy conditions and related with Mt complex assembly/activity impairment in human disease and experimental models. We hypothesize that HHcy inhibits Mt complex I gene expression leading to Mt dysfunction.

Abbreviations: Bet, betaine; BM, bone marrow; C. elegans, caenorhabditis elegans; CBS, cystathionine-β-synthase; CELMP, cardioencephalomyopathy; Cho, choline; CSE, cystathionine γ-lyase; CT, connective tissue; Cysta, cystathionine; D, days; DCC, dog cardiac cells; DD, developmental delay; ELMP, encephalomyopathy; ELP, encephalopathy; Epil, epilepsy; ET, embryonic tissue; ETC, electron transport chain; Exp, expression; GPX, glutathione peroxidase; H2S, hydrogen sulfide; HASMC, human aortic smooth muscle cells; HCM, hypertrophic cardiomyopathy; Hcy, homocysteine; HGNC, HUGO (human gene organisation) gene nomenclature committee; HHcy, hyperhomocysteinemia; HM, high methionine; Hs, homo sapiens; IHF, ischemic heart failure; IM, inner membrane; IMS, intermembrane space; Kid, kidney; LC-ESI-MS/MS, liquid chromatography-electrosprayionization-tandem mass spectrometry; Leigh S, leigh syndrome; LEP, leukoencephalopathy; LN, lymph node; M, matrix; ME, myoclonic epilepsy; Met, methionine; Mm, mus musculus; MNR, mouse neural retina; MRCD, mitochondrial respiratory chain disorder; MT, methyltransferase; Mt, mitochondrial; MtDNA, mitochondrial DNA; Musc, muscle; Mu, mutation; N/A, not analyzed because of lack of EST database profile; ND, not determined; NDD, neurodegenerative disorder; nDNA, nuclear DNA; nMt, nuclear encoded mitochondrial genes; nMt, nuclear encoded mitochondrial genes; nMt-ETC-Com, nuclear-encoded mitochondrial ETC complex; OM, Outer membrane; Ova, Ovary; Panc, Pancreas; PC, Phosphatidylcholine; PE, phosphatidylethanolamine; PG, pituitary gland; SAH, S-adenosylhomocysteine; SAM, S-adenosylmethionine; SMCED, severe muscle complex I enzyme defect; Sple, spleen; STZ, streptozotocin; Tes, testis; Thym, thymus; Tx, treatment

* Corresponding author.
** Corresponding author at: Center for Metabolic Disease Research, Temple University - Lewis Katz School of Medicine, 3500 North Broad Street, Philadelphia, PA 19140, USA.
E-mail addresses: yongji@njmu.edu.cn (Y. Ji), hongw@temple.edu (H. Wang).

https://doi.org/10.1016/j.redox.2018.03.015
Received 8 March 2018; Accepted 22 March 2018
Available online 04 April 2018

1. Introduction

Hyperhomocysteinemia (HHcy) is a significant independent risk factor for cardiovascular disease (CVD) [1,2], stroke [2], neurodegenerative diseases [3,4], diabetes [5,6], kidney dysfunction [7] and a predictor of non-alcoholic liver disease [8]. We and others have reported that HHcy has impact on a variety of biological processes, including suppressing endothelial cell (EC) growth [9,10], promoting vascular smooth muscle cell (VSMC) proliferation, stimulating inflammatory monocytes (MC) differentiation [6,11,12], exacerbating vascular dysfunction, reducing HDL biosynthesis [13,14] and accelerating atherosclerosis [6,11–13,15–17].

It has been suggested that Homocysteine (Hcy) alters Mitochondrial (Mt) biogenesis, gene expression and function in different model systems. Blood Hcy level is negatively correlated with mitochondrial DNA (Mt-DNA) content in WBC in human [18]. HHcy elevated Mt fission protein levels and smaller mitochondria in retinal ganglion cells in mice with cystathionine β-synthase heterozygous deficiency ($Cbs^{+/-}$) [19] and reduced Mt-DNA content in rat tissues [20]. HHcy suppressed Mt respiration, complex IV and SOD2 activity, increased com II activity and ROS generation in myocardial mitochondria [21] and caused cristae disintegration and Mt swelling in cerebrocortical microvascular wall [22] in rats. Further, Hcy (100 μM) increased Mt mass and biogenesis in human EC [23], and Mt electron transport chain (Mt-ETC) genes, and cytochrome c III/Atpase 6, 8 expression in DAMI cells [24]. HHcy increased Mt fission, a process of Mt fragmentation, oxidative phosphorylation (OXPHOS) gene expression, and membrane potential disruption in yeast [25], However, HHcy-induced tissue specific Mt bioenergetics changes and molecular targets have not been well characterized.

The Mt is known as the cell's powerhouse and produces most of the ATP required by most biological processes. ATP is generated through the Mt-ETC. As described in Fig. 1, the Mt-ETC is located in the inner Mt membrane and consists of five complexes, which perform oxidative phosphorylation (OXPHOS) reactions. Complexes I-IV carry a series redox reaction and complex V is responsible for the ATP generation through the phosphorylation of inorganic phosphate. The process also generates ROS for signaling and causing cellular damage in physiological and pathophysiological conditions [26,27]. For example, Mt-ETC disruption results in increased reactive oxygen species (ROS) and oxidative stress [21,23]. Although, Mt have other roles beside energy production well described in [28], the focus of this study is Mt energy and redox homeostasis. Mt-ETC defects are well characterized in Mt disease, which is defined by mtDNA or nDNA mutations, either inherited or spontaneously occurred [29].

Because HHcy causes Mt damage, it is possible that Mt-ETC dysfunction mediates HHcy-induced CVD and other diseases. Despite the fact that nuclear encoded Mt-ETC complex (nMt-ETC-Com) genes, also termed Mt-ETC subunits are thought to be ubiquitously expressed, the tissue expression profile of these genes has not been determined. The relationship of nMt-ETC-Com gene expression with tissue Hcy concentration has not been investigated. The mechanism underlying Hcy-induced Mt dysfunction particularly Mt-ETC has not been elucidated. We hypothesized that Mt-ETC-com genes are responsive to Hcy metabolic changes.

In this study, we employed a set of comprehensive computational database mining analyses previously developed in our lab [30–33] to explore the responsiveness of Mt-ETC to HHcy. We establish tissue expression profiles of the nMt-ETC-Com genes in human and mouse, and assessed tissue Hcy metabolites. The focus and nature of the current study is to combine bioinformatics and metabolic studies, to model Mt ETC and HHcy interactions, and to generate hypotheses for future studies. Our study should provide important insights into the understanding of the role of HHcy in Mt-ETC dysfunction and Mt redox homeostasis.

2. Experimental procedures

2.1. Mt-ETC-com genes and database mining strategies

We selected 97 genes of the Mt-ETC-com, including 44 genes in com I (NADH dehydrogenase (ubiquinone) subunits), 4 genes in com II (succinate dehydrogenase subunits), 10 genes in com III (ubiquinol-cytochrome c reductase complex subunits), 19 genes in com IV (cytochrome c oxidase subunits) and 19 genes in com V (ATP synthase subunits). NCBI/UniGene ID numbers of these genes were obtained from the National Institutes of Health (NIH) and National Center of Biotechnology Information (NCBI) Unigene database (http://www.ncbi.nlm.nih.gov/sites/entrez?db=unigene) as we previously described [30–33] and listed in (Sup. Table 1). Eighty-four nMt-ETC-Com genes were utilized to perform the initial tissue expression and correlation analysis. The MtDNA Mt-ETC-com genes were not included because they did not exist in the EST database. We established tissue expression patterns, profiles and classification of nMt-ETC-Com genes and examined correlation with Hcy metabolites analyzed in mouse tissues listed in (Fig. 2A) by linear regression analysis. In addition, we explored the changes of nMt-ETC-Com genes in experimental models and disease using the NCBI GEO dataset database (http://www.ncbi.nlm.nih.gov/gds/) [34] and literature research. The overall strategy is summarized in Fig. 1.

2.2. Tissue expression pattern, profile and classification of nMt-ETC-Com genes

An experimental data mining strategy was used to assess the tissue expression pattern and profile of mRNA transcript of selected genes as previously described [30–33]. Twenty human and 19 mouse tissues were examined for mRNA expression of selected genes by mining experimentally verified human and mouse Expression Sequence Tag (EST) databases of the National Institutes of Health (NIH)/National Center of Biotechnology Information (NCBI) UniGene (http://www.ncbi.nlm.nih.gov/sites/entrez?db=unigene). Gene mRNA levels are described as gene transcript units per million transcripts (TPM) and normalized with that of β –actin to achieve the relative expression unit (REU). To establish a standard gene expression unit crossing the selected tissues, we calculated the median REU (mREU) from REU in 20 human or 19 mouse selected tissues. The ratio of REU/mREU is expressed as Tissue-median-adjusted mRNA expression levels. A confidence interval of the expression variation of housekeeping genes was generated by calculating the mean plus two times that of the standard deviation of the REU (Mean ± 2 SD) of three selected housekeeping genes: pituitary tumor-transforming 1 interacting protein (PTTG1LP), pyruvate kinase muscle (PKM2), and heterogeneous nuclear ribonucleoprotein K (HNRNPK)(Fig. 4A), as shown in our previous studies [31,33]. In any given tissue, if gene expression levels were above the upper limit of the confidence interval, it was considered as significantly expressed. If zero transcripts per million were detected (REU/mREU = 0), it was considered as undetected and defined as very low expressed and denoted by "-" symbol). Symbol "+" describes genes at REU/mREU > 0 but < upper limit, indicating gene expression level not exceed the housekeeping threshold or upper limit. Symbol "++" describes genes at REU/mREU > upper limit but < 10, and is considered as high expression levels. Symbol "+++" describes genes at REU/mREU > 10 but < 20. Symbol "++++" describes genes at REU/mREU > 20 but < 30. Symbol "+++++" describes genes at REU/mREU > 30 but < 40. Symbol "++++++" describes genes at REU/mREU ≥ 40 as shown in Table 1A and B.

Tissues classification of nMt-ETC-Com genes was established by creating tiers according to the Hcy-suppressive nMt-ETC-Com genes expression pattern in human and mouse (Table 3A and B). Hcy-suppressive genes were obtained from the correlation and simple linear regression analysis.

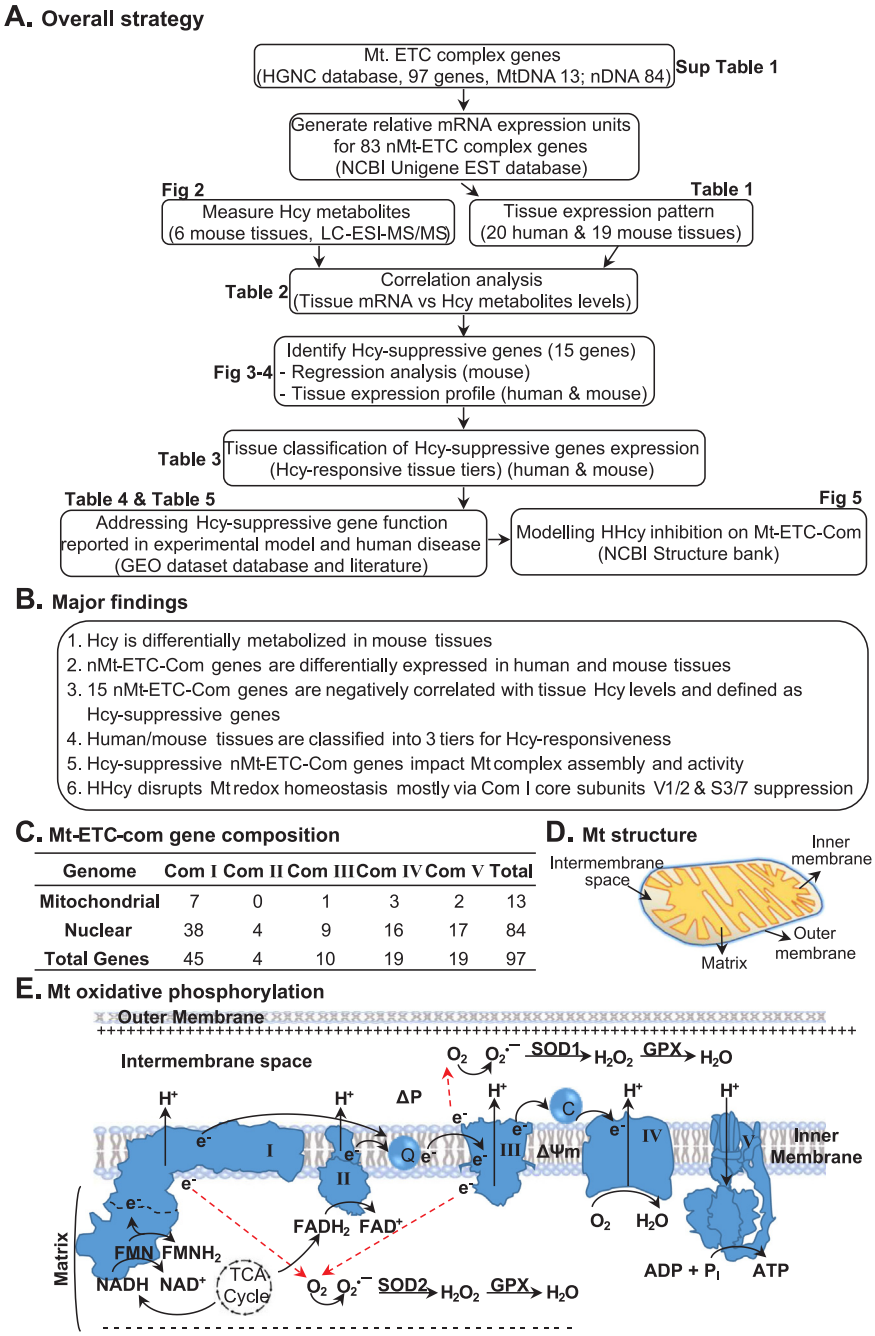

Fig. 1. Research strategy and Mt. ETC complex function and gene composition. A. Overall strategy. Ninety-seven Mt-ETC-com genes were selected from the HGNC database (13 encoded by MtDNA, 84 encoded by nDNA). mRNA expression patterns of these genes were established in 20 human & 19 mouse tissues by using the NCIB Unigene EST database. Hcy metabolites were measured in six tissues from C57/B6 mice (heart, liver, lung, kidney, spleen and brain) by LC-ESI-MS/MS. Correlation analysis between tissue mRNA and Hcy metabolite levels was performed. Fifteen Mt-ETC-com genes were identified as Hcy-suppressive genes. Their tissue expression profile was established in human and mouse. Correlation of nMt-ETC-Com genes mRNA with Hcy and metabolites in mouse tissues was determined by regression analysis. Hcy-responsive tissue tiers were established. Hcy-suppressive gene changes in experimental models (GEO dataset database) and disease (literature research) were explored. B. Major findings. Summary of major discoveries in this study. **C. Mt-ETC-com gene composition.** Mt-ETC-com are composed of 97 proteins, 13 of which are encoded by the Mt genome and 84 of which are encoded by nuclear genome. **D. Mt structure.** Mt structure showing names of its different parts. E. Mt oxidative phosphorylation. Mt-ETC consists of five complexes (I-V) residing on the inner mitochondrial membrane. Throughout mitochondrial respiration, the TCA cycle, taking place in the Mt matrix, provides reduced molecules NADH and FADH2, which serve as electron (e^-) donors to complex I and II, respectively. These electrons are transferred to coenzyme Q (Q), and then to complex III. Cytochrome C (C) accepts the electrons from complex III and then transports them to complex IV, wherein molecular oxygen is reduced to water. The redox reactions through complex I to IV result in hydrogen ion (H^+, protons) transferred to Mt intermembrane space, which creates a hydrogen gradient/motive proton force (Δp) and mitochondrial innermembrane potential (ΔΨm). The Δp pumps the H^+ back to the matrix and facilitate ADP phosphorylation using inorganic phosphate for ATP synthesis. In a physiological setting, electrons leak from complex I to the matrix and from complex III to the intermembrane space and matrix (indicated by dashed arrows). These electrons can react with molecular oxygen (O_2) to produce superoxide anions ($O_2^{\cdot-}$), which are rapidly dismutated by superoxide dismutase (SOD), SOD2 in the matrix and SOD1 in the intermembrane space, to form hydrogen peroxide (H_2O_2). Glutathione peroxidase (GPX) reduces H_2O_2 to water and relieves oxidative stress.

2.3. Tissue Hcy metabolites measurements in mouse

The concentration of Hcy, SAM and SAH was measured in six tissues (heart, liver, lung, kidney, spleen and brain) in C57BL/6 J (n = 4) mice from 13.4 to 18 weeks of age. Metabolic connection of these metabolites was described in Fig. 2. Mouse tissues were collected and homogenized in 4 M perchloric acid (PCA) solution. The homogenized tissue was centrifuged for 10 min at 2000 rpm. Supernatant was collected and stored at − 80°C. Metabolite levels were analyzed by liquid chromatography-electrospray ionization-tandem mass spectrometry (LC-ESI-MS/MS) and presented in Fig. 2A.

2.4. Correlation and simple linear regression analysis and Hcy-suppressive gene identification

Correlation and simple linear regression analysis of gene expression with metabolites was performed by plotting mRNA levels (REU) of nMt-ETC-Com genes vs Hcy metabolites (SAM, SAH and SAM/SAH) concentration levels in 6 mouse tissues (heart, liver, lung, kidney, spleen and brain) (Fig. 2A) as previously described [31,32]. This analysis allowed us to identify the Hcy-suppressive genes, which are negatively correlated with Hcy metabolites (Fig. 3). Symbols were used to define the correlation type; "-" for negative correlation, "+" for positive correlation and " ± " for no correlation (Table 2).

2.5. Hcy-suppressive gene screening in experimental and disease studies

The identified Hcy-suppressive nMt-ETC-Com genes were screened in three HHcy-related microarray analyses in the Gene Expression Omnibus (GEO) dataset databases (GSE9490, GSE56458 and GSE5260) (Table 4) [34]. The GEO is an international public functional genomics data repository that freely distributes microarray, next-generation

A. Hcy metabolite levels in mouse tissues (nmol/g wet tissue)

Metabolites / Tissue	HCY	SAM	SAH	SAM:SAH
KIDNEY	23.7±18.5	28.8±6.5	32.9±6.5	0.9±0.2
LUNG	23.3±4.7	41.9±7.1	7.01±7.1	6.2±1.4
SPLEEN	20.0±10.5	38.0±6.4	1.6±6.4	25.6±5.9
LIVER	14.3±13.9	28.8±10.5	58.7±10.5	0.6±0.3
BRAIN	5.4±3.3	18.2±3.0	4.3±1.2	4.7±1.8
HEART	4.6±2.5	32.6±4.4	5.1±4.4	6.5±1.5

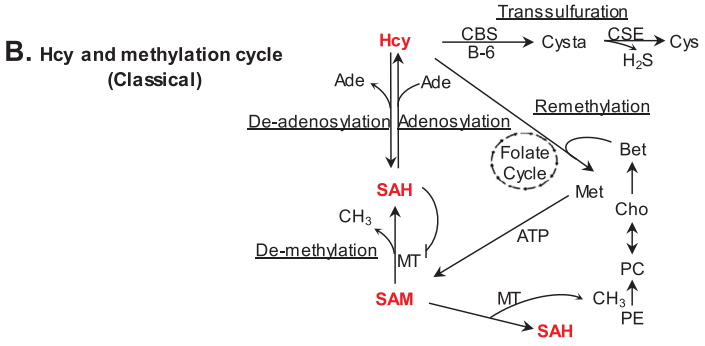

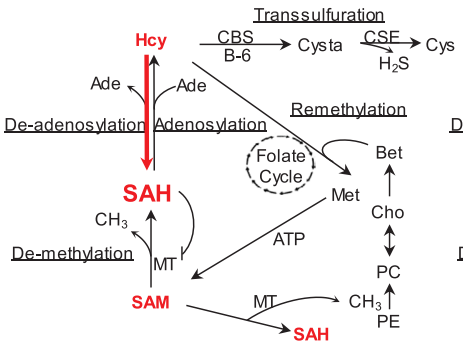

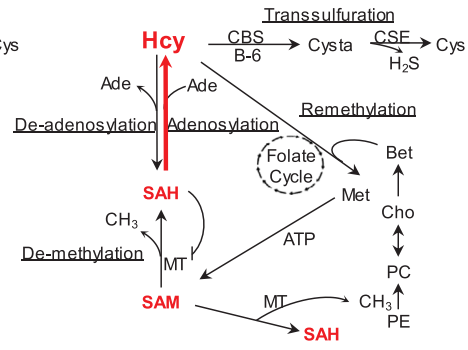

Fig. 2. Hcy and methylation cycle - Mouse tissue Hcy metabolites. A. Hcy metabolite levels in mouse tissues. Hcy metabolites were measured in six tissues (heart, liver, lung, kidney, spleen, and brain) from C57BL/6 J mice (n = 4, 14–18 weeks of age). Samples were collected and homogenized with 4 M perchloric acid (PCA) solution. Tissues extracts were assessed for Hcy metabolites (Hcy, SAM and SAH) by LC-ESI-MS/MS as described in the materials and methods section. B. Hcy and methylation cycle (Classical) Hcy is generated by Met demethylation and de-adenosylation. Hcy can be removed by the transsulfuration pathway to generate Cysta, Cys, H2S and others by-products, or be re-methylated back to Met by receiving a methyl group from the folate cycle and/or Cho-Bet metabolism. Through adenosylation, Hcy can form SAH, a potent inhibitor of nuclear methylation. SAM is converted from Met metabolism in an ATP dependent manner and serves as a methyl donor for PE to PC conversion, which can also come from phosphorylation of Cho, a precursor of Bet. C/D. Hcy and methylation cycle (Liver/Spleen). Representation of tissue specific Hcy-SAH metabolic models.

sequencing, and other forms of high-throughput functional genomics data submitted by the research community. GEO allows one to analyze data using the GEO2R tool, which uses R software for statistical analysis. The impact of these genes in Mt complex activity and assembly were also summarized through literature research in PubMed reported experimental and disease studies (Table 5).

2.6. Modelling HHcy inhibition on Mt-ETC-Com genes

Hcy-suppressive nMt-ETC-Com genes were modeled using information from single-particle cryo-electron microscopy (cryo-EM) structure analysis from the NCBI Structure bank in a Com I 3D sphere structure model [35] visualized using Cn3D 4.3.1. Software [83].

3. Results

3.1. Hcy and methylation-related metabolites were differentially distributed among mouse tissues

We examined the levels of Hcy metabolites, including S-adenosylmethionine (SAM) and S-adenosylhomocysteine (SAH) in 6 tissues (heart, liver, lung, kidney, spleen and brain) in wild type C57BL/6 J mice by using LC-ESI-MS/MS. Hcy levels were high in the kidney, lung, spleen and liver (ranging from 23.7 to 14.3 nmol/g tissue), but low in brain and heart (around 5.4–2.9 nmol/g tissue). SAM concentrations were relatively consistent in all tissues examined (41.9–18.2 nmol/g tissue). SAH levels were relatively high in the liver and kidney (58.7 and 32.9 nmol/g tissue) and low in lung, heart, brain and spleen (ranging from 7 to 1.6 nmol/g tissue). SAM/SAH ratio was high in the spleen (25.6), heart, lung and brain (ranging from 6.5 to 4.7), and very low in the kidney and liver (0.9–0.6) (Fig. 2A). Using highest and lowest SAH-containting tissues, liver and spleen, respectively, we established a tissue specific Hcy-SAH metabolic model which is presented in Fig. 2C/D.

3.2. nMt-ETC-Com genes are differentially expressed in human and mouse tissue

We established nMt-ETC-Com genes expression profile in 20 human and 19 mouse tissues summarized in Table 1A and B. Although nMt-ETC-Com genes were broadly expressed in all human and mouse tissues, their expression pattern appeared to be different between tissues and species. Undetected genes were defined as very low expressed and denoted by "-", whereas the detectable but under the upper limit of confidence interval genes were denoted as "+". Gene expression that exceeded the upper limit of the confidence interval was defined as "++" and justified by statistical significance. The highest expressed genes were denoted by "++++++".

In human tissues, nMt-ETC-Com genes were expressed across most of the tissues. Muscle, pituitary gland (PG) and heart were most abundant for nMt-ETC-Com gene expression and had 84.6%, 67.9% and 57.7% of 78 nMt-ETC-Com genes expressed at high levels (++ or more), respectively. Other tissues were relatively less abundant for nMt-ETC-Com gene expression, such as bone marrow (BM) 19%, eye 17.9%, liver 14.1% and pancreas 11.5%.

In mouse tissues, nMt-ETC-Com genes were broadly expressed. Heart, pancreas, lymph node (LN) and muscle were most abundant for nMt-ETC-Com gene expression and had 58.7%, 49.3%, 42.7% and 32%

Table 1A
Tissue expression pattern of nMt ETC complex genes in 20 human tissues.

Genes ID# names	Tissues	Blood	Bone	BM	Brain	CT	ET	Eye	Heart	Kid	Liver	Lung	LN	Musc	Ova	Panc	PG	Sple	Tes	Thym	Vasc
Mitochondrial Complex I: NADH dehydrogenase (ubiquinone) subunits (45):																					
8	NDUFA1	+	+	++	+	+	+	+	+++	+	+	+	+	+++++	+	+	++	+	+	-	+
9	NDUFA2	+	+	+	+	+	+	+	++	+	+	+	+	++	+	+	+++++	-	+	-	+
10	NDUFA3	+	+	+++	+	-	+	+	+	+	+	+	-	++++	+	+	+++	-	+	-	+
11	NDUFA4*	+	+	++	+	+	+	++	+++	+	++	+	+	+++	+	+	++	+	+	+	++
12	NDUFA5	+	+	++	+	+	+	+	+	+	+	+	+	+++	+	+	++	-	+	+	+
13	NDUFA6	+	+	++	+	+	+	+	++	+	+	+	+	++++	+	+	-	-	+	+	+
14	NDUFA7	+	+	++	+	-	+	+	++	+	+	+	+	+++	+	+	++	+	+	+	+
15	NDUFA8	+	+	+	+	+	+	+	++	+	+	+	-	++	+	+++	+++	-	+	+	-
16	NDUFA9	+	+	+	+	+	+	+	+	+	+	+	+	+++	+	+	+++	+	+	+	+
17	NDUFA10	+	+	+	+	+	+	+	+	+	+	+	+	+	+	+	+	+	+	+	+
18	NDUFA11	+	+	+	+	-	+	++	+	+	+	+	+	++++	+	+	+++	+	+	+	+
19	NDUFA12	+	+	+	+	+	+	+	++	+	+	+	+	+++	+	+	++	-	+	-	+
20	NDUFA13	+	+	+	+	+	+	+	++	+	+	+	+	+++	+	+	+++	+	+	+	+
21	NDUFAB1	+	+	+	+	+	+	+	+	+	+	+	+	++	+	++	+	-	+	-	+
22	NDUFB1	+	+	+	+	++	+	+	+	+	+	+	-	++	+	+	+++++	-	+	-	+
23	NDUFB2	+	+	+	+	+	+	+	++	+	+	+	-	++++	+	+	++++	-	+	-	-
24	NDUFB3	+	+	+	+	+	+	+	++	+	+	+	-	+++	+	+	-	+	+	-	+
25	NDUFB4	+	+	++	+	+	+	+	+	+	+	+	+	++++	+	+	++	-	+	+	+
26	NDUFB5	+	+	++	+	+	+	+	+	+	+	+	+	+++	+	+	-	-	+	-	+
27	NDUFB6	+	+	+	+	+	+	+	++	+	+	+	+	+	-	+	++	-	+	-	+
28	NDUFB7	+	+	+	+	-	+	+	+	+	+	+	+	++	+	+	++++	+	+	-	-
29	NDUFB8	+	+	+	+	+	+	+	+	+	+	+	+	++	+	+	+	+	+	+	+
30	NDUFB9	+	+	+	+	+	+	+	+	+	+	+	+	+++	+	+	+	-	+	+	+
31	NDUFB10	+	+	+	+	+	+	++	+	+	+	+	+	++++	+	+	+++	-	+	-	+
32	NDUFB11	+	+	+	+	+	+	++	++	+	+	+	++	+++	+	+	++	+	+	+	-
33	NDUFC1	+	-	+	+	+	+	++	+	++	+	+	+	+++	+	+	++++	-	+	-	+
34	NDUFC2	+	+	+	+	+	+	+	+	+	+	+	+	+	+	+	+++	-	+	+	+
35	NDUFS1	+	++	++	+	+	+	+	+	+	+	+	+	+++++	+	+	-	-	+	-	+
36	NDUFS2	+	+	+	+	+	+	+	+	+	++	+	+	++	+	+	-	+	+	+	-
37	NDUFS3	+	+	-	+	+	+	+	++	+	+	+	+	++	+	++	++	+	+	+	+
38	NDUFS4	+	+	-	+	++	+	++	+++	+	+	+	+	++	+	++	-	-	+	-	+
39	NDUFS5	+	+	+	+	+	+	++	++	+	+	+	+	+++	+	+	++	+	+	+	+
40	NDUFS6	+	+	+	+	+	+	+	++	+	++	+	++	+++	+	+	-	+	+	-	+
41	NDUFS7	+	-	-	+	+	+	++	+	+	+	+	-	++++	+	+	-	+	+	+	-
42	NDUFS8	+	+	-	+	+	+	++	+	+	++	+	+	++	+	+	++	+	+	+	+
43	NDUFV1	+	+	+	+	+	+	+	++	+	+	+	+	++	+	+	+	+	+	+	+
44	NDUFV2	+	+	-	+	++	+	+	+	+	+	+	+	++	+	+	++	+	+	+	+
45	NDUFV3	+	+	+	+	+	+	+	++	+	+	+	+	++	+	+	-	+	+	-	++
Mitochondrial Complex II: succinate dehydrogenase subunits (4):																					
46	SDHA	+	+	+	+	+	+	+	++	+	+	+	+	++	+	+	+	+	+	+	+
47	SDHB	+	+	+	+	+	+	+	+	+	+	+	-	++	+	+	++	-	+	-	+
48	SDHC	+	+	+	+	+	+	+	+	+	+	+	+	+	+	+	++	+	+	+	+
49	SDHD	+	+	++++	+	+	+	+	+	+	++	+	+	+++	+	+	++	-	+	-	+
Mitochondrial Complex III: ubiquinol-cytochrome c reductase complex subunits (10):																					
50	CYC1	+	+	+	+	+	+	+	+	+	+	+	+	+++	+	++	-	-	+	+	+
52	UQCR10	+	-	+	+	+	+	+	++	+	++	+	+	++++	+	+	++++	+	+	+	+
53	UQCR11	+	+	+	+	+	+	+	++	+	+	+	+	++++	+	+	-	+	+	-	+
54	UQCRB	+	++	+	+	+	+	+	++	+	+	+	+	++++	+	+	+++	+	+	-	+
55	UQCRC1	+	+	+	+	+	+	+	+	+	+	+	+	++	+	+	++	+	+	+	+
56	UQCRC2	+	+	+	+	+	+	+	++	+	+	+	+	++	+	+	++	+	+	+	+
57	UQCRFS1	+	+	+	+	+	+	+	++	+	+	+	+	++	+	+	-	+	+	-	+
58	UQCRH	+	+	+	+	+	+	+	+	+	+	+	+	++	+	+	++	+	+	+	+
59	UQCRQ	+	+	++	+	+	+	++	+++	+	++	+	+	++++	+	+	+++	+	+	+	+

Mitochondrial Complex IV: cytochrome c oxidase subunits (19):																				
60	COX4I1	+	+	+	+	+	+	+	++	+	+	+	+	++	+	+	++	+	+	+	+
61	COX4I2	-	-	-	-	-	-	-	-	-	-	-	-	-	-	-	-	-	-	-	-
62	COX5A	+	+	+	+	+	+	+	+	+	+	+	++	+++	+	++	-	+	+	-	-
63	COX5B	+	+	+	+	+	+	+	++	+	+++	+	+	+++++	+	++	++++	+	+	-	+
64	COX6A1	+	+	+	+	+	+	+	++	+	+	+	+	+	+	+	++	+	+	+	+
65	COX6A2	-	-	-	-	-	-	-	-	-	-	-	-	-	-	-	-	-	-	-	-
66	COX6B1	+	+	+	+	+	+	+	++	+	+	+	+	++++	+	+	+	+	+	+	+
67	COX6B2	-	-	-	-	-	-	-	-	-	-	-	-	-	-	-	-	-	-	-	-
68	COX6C	+	+	+	+	+	+	+	++	+	+	+	+	+++	+	+	++	-	+	+	+
69	COX7A1	-	+	-	+	-	+	++	+++++	++	-	+	-	++++++	-	+	+++++	+	+	-	+
70	COX7A2	+	+	+	+	+	+	+	++	+	+	+	+	++	-	+	+++++	-	+	+	+
71	COX7B	+	+	++	+	+	+	+	+++	+	++	+	+	+++++	+	+	-	+	+	+	+
72	COX7B2	-	-	-	-	-	-	-	-	-	-	-	-	-	-	-	-	-	-	-	-
73	COX7C	+	+	+	+	+	++	+	++	+	+	+	+	++++	+	+	+++	+	+	-	+
74	COX8A	+	+	+	+	+	+	++	+++	+	+	+	+	++++	+	+	++	-	+	+	+
75	COX8C	-	-	-	-	-	-	-	-	-	-	-	-	-	-	-	-	-	-	-	-
Mitochondrial complex V: ATP synthase subunits (19):																				
79	ATP5A1	+	+	+	+	+	+	++++	+++	+	+	+	+	++	+	+	++	+	+	+	+
80	ATP5B	+	+	+	+	+	+	+	+	+	+	+	+	++	+	+	++	+	+	+	+
81	ATP5C1	+	+	++	+	+	+	+	+	+	+	+	+	+++	+	+	++	+	+	+	+
82	ATP5D	+	++	+	+	+	+	++	+	+	+	++	+	++++++	+	+	+++	+	+	-	-
83	ATP5E	+	+	+	+	-	+	+	++	+	+++	+	+	+++	+	+	++++	+	+	+	++
84	ATP5F1	+	+	+	+	+	+	+	+	+	+	+	+	+++	+	+	++	+	+	+	+
85	ATP5G1	+	+	+	+	+	+	+	++	+	+	+	+	++	+	+	++	-	+	+	+
86	ATP5G2	+	+	+	+	+	+	+	++	+	+	+	+	+++	+	+	++	+	+	+	+
87	ATP5G3	+	+	+	+	+	+	+	++	+	+	+	+	+	+	+	+	+	+	+	+
88	ATP5H	+	+	+	+	+	+	+	+	+	+	+	+	+	-	++	+	+	++	+	+
89	ATP5I	+	-	+	+	-	+	+	+	+	++	+	-	++	-	+	++	+	+	+	+
90	ATP5J	+	+	+	+	+	+	+	+++	+	+	+	+	+	-	+	+++	+	+	+	+
91	ATP5J2	+	+	++	+	+	+	+	++	+	+	+	-	+	+	++++	-	+	+	+	+
92	ATP5L	+	+	++	+	+	+	+	++	+	+	+	+	+	+	+	++	+	+	+	+
93	ATP5L2	-	-	-	-	-	-	-	-	-	-	-	-	-	-	-	-	-	-	-	-
94	ATP5O	+	+	+	+	+	+	+	++	+	+	+	+	+	+	+	++	+	+	+	+
95	ATPIF1	+	+	+	+	+	+	+	++	+	+	+	+	+	-	+	-	+	+	+	+
Expressed genes (%)		98.7	94.9	92.3	100	91	100	100	100	100	98.7	100	87.2	100	91	100	79.5	67.9	100	65.4	89.7
Highly expressed genes (%)		0	3.8	19.2	0	3.8	1.3	17.9	57.7	1.3	14.1	1.3	3.8	84.6	0	11.5	67.9	0	1.3	0	3.8

Table 1B
Tissue expression pattern of nMt ETC complex genes in 20 mouse tissues.

Genes ID# names	Tissues	Blood	Bone	BM	Brain	CT	ET	Eye	Heart	Kid	Liver	Lung	LN	Musc	Ova	Panc	PG	Sple	Tes	Thym
Mitochondrial Complex I NADH dehydrogenase (ubiquinone): subunits (45):																				
8	NDUFA1	-	-	+	++	-	+	+	++	+	++	+	+++	-	+	++	+++	+	+	+
9	NDUFA2	+	-	+	+	+	+	+	+	+	+	+	++	+	+	+	+	+	+	+
10	NDUFA3	-	-	-	++	-	+	+	++	+	++	-	+++++	+	-	+++	-	+	++	+
11	NDUFA4*	+	+	-	++	-	+	+	++	+	+	+	++	+	-	++	-	+	+	+
12	NDUFA5	+	-	+	++	+	+	+	++	+	+	+	-	++	-	++	-	-	++	+
13	NDUFA6	+	-	+	+	-	+	+	++	+	+	+	+++	-	-	++	-	+	++	++
14	NDUFA7	-	-	+	+	-	+	+	++	+	++	-	+++	++	+	++	-	+	++	+
15	NDUFA8	+	+	+	+	+	+	+	++	+	+	+	-	+	+	-	+	+	+	+
16	NDUFA9	+	-	+	+	+	+	+	+	+	+	+	+++	+	+	+	+	+	+	+
17	NDUFA10	+	+	+	+	+	+	+	++	+	+	+	+	+	+	+	+	+	+	+
18	NDUFA11	-	-	-	+	-	+	+	+	+	+	+	++	+	-	+	-	+	+	+
19	NDUFA12	+	-	+	+	-	+	+	+	+	+	-	+	+	-	++	-	+	+	+
20	NDUFA13	-	+	+	++	-	+	+	+	+	+	+	-	+	+	++	++	+	++	+
21	NDUFAB1	+	+	+	+	-	+	+	+	+	+	+	++++	+	+	++	-	+	+	++
22	NDUFB1	-	-	-	-	-	-	-	-	-	-	-	-	-	-	-	-	-	-	-
23	NDUFB2	+	+	+	++	-	+	+	++	+	++	+	-	-	-	+++	-	+	+	+
24	NDUFB3	+	-	+	+	+	+	+	+	+	+	+	-	++	-	+	++	+	+	+
25	NDUFB4	+	-	+	+	-	+	+	+	+	+	-	++	+	+	++	+	-	+	+
26	NDUFB5	+	-	+	+	-	+	+	++	+	+	+	+	+	+	+	-	+	+	+
27	NDUFB6	-	+	+	+	-	+	+	++	+	+	+	++	-	-	+	-	+	+	+
28	NDUFB7	+	+	+	+	+	+	+	+	+	+	+	-	++	+	+	-	+	+	+
29	NDUFB8	+	+	+	+	+	+	+	+	+	+	+	++	+	-	++	+	+	+	+
30	NDUFB9	-	-	+	+	+	+	+	++	+	+	+	-	++	+	++	++	+	+	+
31	NDUFB10	-	-	+	+	+	+	+	+	+	+	+	-	++	+	+	-	+	+	+
32	NDUFB11	+	-	+	+	+	+	+	+	+	+	+	-	++	+	++	++	+	+	+
33	NDUFC1	+	-	+	++	-	+	+	++	+	+	+	-	+	+	+	-	+	+++	+
34	NDUFC2	+	+	+	+	-	+	+	+	+	+	+	++	+	+	++	++	++	+	+
35	NDUFS1	+	-	+	+	-	+	+	+	+	+	+	+++	+	+	++	-	+	+	+
36	NDUFS2	+	+	+	+	+	+	+	++	+	+	+	-	+	+	+	+	+	+	+
37	NDUFS3	+	-	+	+	-	+	+	+	+	+	+	++	++	-	+	++	+	+	+
38	NDUFS4	-	-	+	+	-	+	+	+	+	+	+	++++	+	+	+	+++	+	+	+
39	NDUFS5	-	+	+	++	-	+	+	+	+	++	-	+++	+++	-	++	++++	-	+++	++
40	NDUFS6	-	-	+	+	-	+	+	++	+	++	-	-	+	+	+++	-	+	++	+
41	NDUFS7	-	+	+	+	-	+	+	+	+	+	+	-	++	+	++	++	+	+	+
42	NDUFS8	+	-	+	+	-	+	+	+	+	+	+	+	+	+	+	-	+	+	+
43	NDUFV1	+	+	+	+	+	+	+	+	+	+	+	-	+	+	+	+	+	+	+
44	NDUFV2	+	+	+	+	+	+	+	++	+	+	+	-	++	+	+	-	+	++	+
45	NDUFV3	+	-	+	+	+	+	+	+	+	+	+	+	+	+	++	-	+	+	+
Mitochondrial Complex II succinate dehydrogenase subunits (4):																				
46	SDHA	+	+	+	+	+	+	+	+	+	+	+	+	+	+	+	++	+	+	+
47	SDHB	+	-	+	+	-	+	+	++	+	+	+	++	++	-	++	+	+	+	+
48	SDHC	+	+	+	+	+	+	+	++	++	++	+	++	+	+	+	+	+	+	+
49	SDHD	+	+	+	+	+	+	+	++	+	+	+	-	++	+	+	++	+	+	+
Mitochondrial Complex III ubiquinol-cytochrome c reductase complex subunits (10):																				
50	CYC1	-	+	+	+	+	+	+	+	+	+	+	+	+	-	+	+	+	+	+
52	UQCR10	+	-	-	+	+	+	+	++	+	+	-	++	+	-	++	-	+	+	+
53	UQCR11	-	+	+	++	+	+	+	++	+	++	+	+++	-	+	++	++	+	+	+
54	UQCRB	-	-	+	+	-	+	+	++	+	+	-	++	+	+	++	++	+	++	+
55	UQCRC1	+	+	+	+	+	+	+	++	+	+	+	-	++	+	+	-	+	+	+
56	UQCRC2	+	+	+	+	+	+	+	+	+	+	+	++	+	++	+	+++	+	+	+
57	UQCRFS1	+	+	+	+	+	+	+	++	+	+	+	++	++	+	+	+	+	+	+
58	UQCRH	+	+	+	+	+	+	+	+	+	+	+	+	+	+	++	+	+	+	+
59	UQCRQ	+	-	+	+	-	+	+	+	+	++	+	++	+	+	++	-	+	++	+

Mitochondrial Complex IV cytochrome c oxidase subunits (19):																					
60	COX4I1	+	+	+	+	+	+	+	++	+	+	+	-	++	+	+	+	+	++	+	
61	COX4I2	-	-	-	-	-	-	-	-	-	-	-	-	-	-	-	-	-	-	-	
62	COX5A	+	+	+	+	+	+	+	++	+	+	+	+	++	+	++	-	+	++	+	
63	COX5B	-	-	+	+	-	+	+	+	+	+	+	-	+	+	+	-	+	++	-	
64	COX6A1	+	+	+	+	+	+	+	+	+	+	+	-	+	+	++	-	+	+	+	
65	COX6A2	-	-	-	-	-	-	-	-	-	-	-	-	-	-	-	-	-	-	-	
66	COX6B1	+	-	+	+	-	+	+	++	+	+	+	-	+	+	++	+	+	+	+	
67	COX6B2	-	-	-	-	-	-	-	-	-	-	-	-	-	-	-	-	-	-	-	
68	COX6C	-	+	+	+	+	+	+	++	+	+	+	-	++	+	+	+	+	++	+	
69	COX7A1	-	-	-	-	-	-	-	-	-	-	-	-	-	-	-	-	-	-	-	
70	COX7A2	+	-	+	+	-	+	+	++	+	+	+	+	-	+	+	-	+	++	+	
71	COX7B	+	+	+	+	+	+	+	++	+	+	-	++	++	+	++	-	+	+	+	
72	COX7B2	-	-	-	-	-	-	-	-	-	-	-	-	-	-	-	-	-	-	-	
73	COX7C	+	-	+	+	-	+	+	++	+	+	+	++	+	+	++	-	+	+	+	
74	COX8A	+	-	+	+	+	+	+	+	+	+	+	++	+	-	++	-	+	+	+	
75	COX8C	-	-	-	-	-	-	-	-	-	-	-	-	-	-	-	-	-	-	-	
Mitochondrial complex V ATP synthase subunits (19):																					
79	ATP5A1	+	+	+	+	+	+	+	++	+	+	+	+	+	+	+	+	+	+	+	
80	ATP5B	+	+	+	+	+	+	+	++	+	+	+	+	+	+	+	+	+	+	+	
81	ATP5C1	+	+	+	+	+	+	+	++	+	+	+	-	++	+	+	+	+	+	+	
82	ATP5D	+	+	+	+	-	+	+	++	+	++	+	-	++	-	+	++	+	+	+	
83	ATP5E	-	+	-	+	+	+	+	++	+	+	-	++	+	+	++	-	+	++	+	
84	ATP5F1	+	+	+	+	+	+	+	++	+	+	+	+	+	+	+	+	+	+	+	
85	ATP5G1	+	-	-	+	+	+	+	++	++	+	+	-	+	-	+	-	+	+	+	
86	ATP5G2	+	+	+	+	-	+	+	+	+	+	+	-	+	+	+	+	+	+	+	
87	ATP5G3	+	-	+	+	-	+	+	+	+	+	+	+	++	+	+	++	+	+	+	
88	ATP5H	+	+	+	+	-	+	+	++	+	+	-	-	++	+	+	-	+	+	+	
89	ATP5I	N/A	N/A	N/A	N/A	N/A	N/A	N/A	N/A	N/A	N/A	N/A	N/A	N/A	N/A	N/A	N/A	N/A	N/A	N/A	
90	ATP5J	+	+	+	+	+	+	+	++	+	+	+	++	+	+	+	-	+	+	+	
91	ATP5J2	-	-	+	+	-	+	+	++	+	+	+	-	+	+	++	+	+	+	+	
92	ATP5L	+	-	+	+	+	+	+	++	+	++	+	++	+	+	++	-	+	+	+	
93	ATP5L2	-	-	-	-	-	-	-	-	-	-	-	-	-	-	-	-	-	-	-	
94	ATP5O	+	-	+	+	+	+	+	++	+	+	+	-	++	+	++	+	+	+	+	
95	ATPIF1	+	-	+	+	+	+	+	+	+	+	+	++	+	+	++	++	+	++	-	
Expressed genes (%)		74.7	50.7	92.0	100	55	100	100	100	100	100	85	61.3	92	76	99	54.7	96	100	97.3	
Highly expressed genes (%)		0	0	0	12	0	0	0	57.3	2.7	14.7	0	42.7	32	1.3	49	24	1.3	24	4	

Table 1. Tissue expression pattern of nMt-ETC-Com genes (subunits). Twenty human and 19 mouse tissues were examined for mRNA expression by mining EST databases in the NCBI-UniGene site (http://www.ncbi.nlm.nih.gov/unigene). Tissue mRNA levels of nMt ETC complex genes were calculated as REU/mREU, and the confidence interval of housekeeping genes mRNA expression was established, as described in the section of Method and Fig. 4. A. Tissue expression pattern in 20 human tissues. B. Tissue expression pattern in 19 mouse tissues. Symbols were used to define mRNA expression levels based on REU/mREU. Tissue abundances of nMt-ETC-Com genes are described as the ratio percentage of highly expression genes. Symbols were assigned to describe gene expression. Genes were excluded if expression level is recorded as "-" in all tissues. "-", undetected (very low expression) (REU/mREU 0); "+", (> 0) but less than the upper limit; "++", greater than the upper limit but < 10; "+++", > 10 but < 20; "++++", > 20 but < 30; "+++++", > 30 but < 40 and "++++++", ≥40. Abbreviation: N/A, Not analyzed because of lack of EST database profile; nMt, nuclear encoded mitochondrial genes; BM, Bone marrow; CT, Connective tissue; ET, Embryonic tissue; Kid, Kidney; LN, Lymph node; Musc, Muscle; Ova, Ovary; Panc, Pancreas; PG, Pituitary gland; Sple, Spleen; Tes, Testicle; Thym, Thymus. ***NDUFA4 was initially included, but is lately not considered as a Com I subunit.**

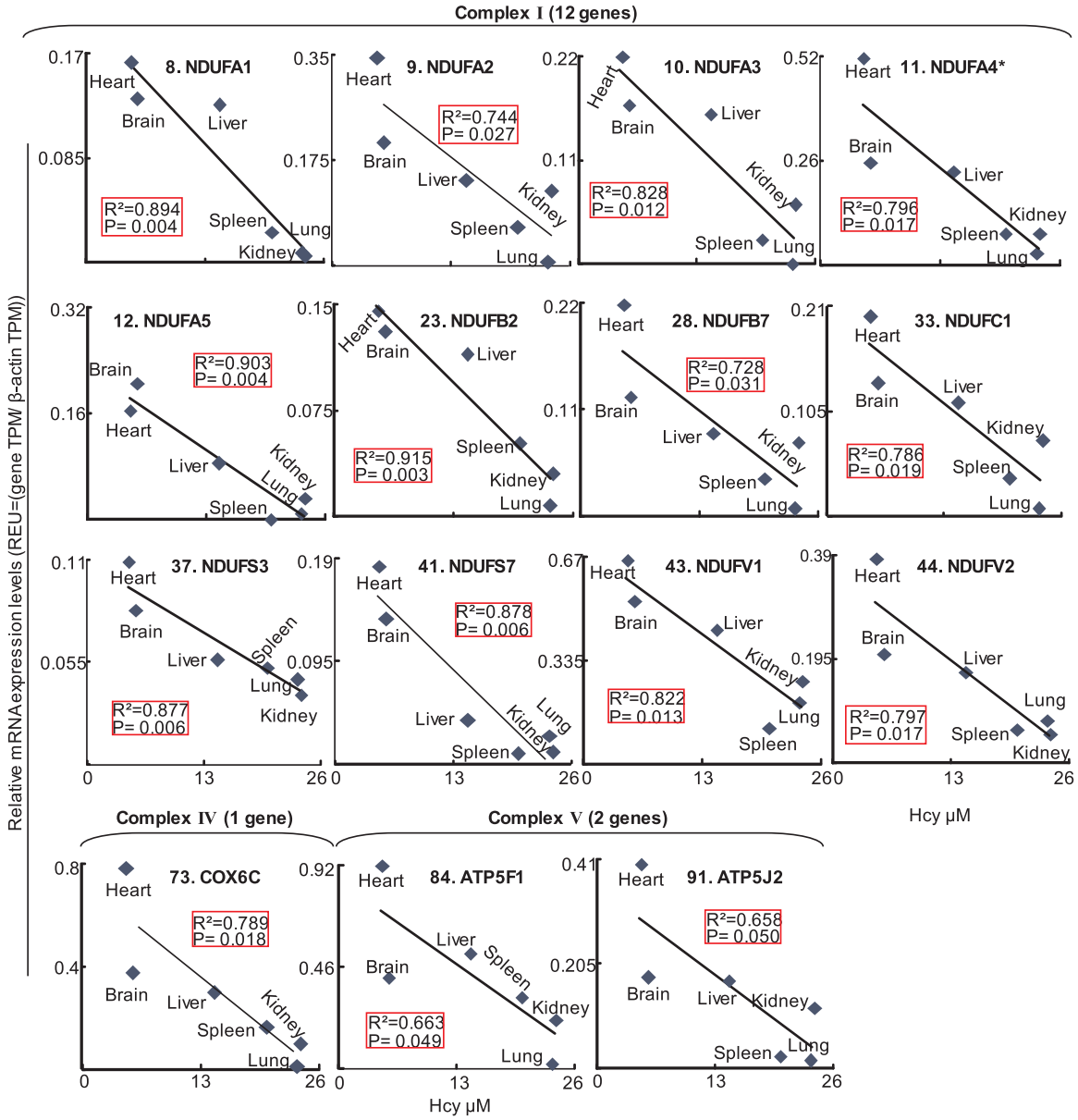

Fig. 3. Simple linear regression of nMt-ETC-Com genes mRNA with Hcy levels in mouse tissues. Linear regression between 84 nMt-ETC-Com gene mRNA and Hcy levels in 6 mouse tissues (heart, liver, lung, kidney, spleen and brain) was performed. Relative expression units (REU) of selected genes were determined as described in (Fig. 4). Tissue REU of genes mRNA were plotted against tissue Hcy levels shown in (Table 2). Among the 84 nMt-ETC-Com genes, the expression of 15 genes was negatively correlated with Hcy levels in normal mouse tissue (Table 3). * NDUFA4 was initially included, but is lately not considered as a Com I subunit.

of 75 nMt-ETC-Com genes expressed at high levels (+ + or more), respectively. Other tissues were relatively less abundant for nMt-ETC-Com gene expression, such as pituitary gland, testis, liver and brain which had 24%, 24%, 14.7% 12% of 75 nMt-ETC-Com genes expressed at high levels (+ + or more), respectively.

Heart and muscle were among the tissues which were most abundant for nMt-ETC-Com gene expression in both humans and mice. Heart and liver nMt-ETC-Com gene abundance was not different between human and mice tissues (57.7% and 14.1% in human, 58.7% and 14.7% in mice). Human heart and liver seem to have different nMt-ETC-Com subunit selection and have relatively higher expression level (eight and two genes were expressed at + + + or higher in human heart and liver). Interestingly, human muscle and pituitary gland tissues were much more abundant for nMt-ETC-Com gene expression than mouse muscle and PG tissues (84.6% vs 32% and 67.9% vs 24%). More interestingly, we found that human BM and eye tissues had more nMt-ETC-Com genes expressed at high levels than that in mice (19.2% and 17.9% in human vs 0% and 0% in mice). Furthermore, mouse lymph node, testis and brain had more nMt-ETC-Com genes expressed at high levels than that in humans (42.7%, 24% and 12% in mice vs 3.8%, 1.3% and 0% in human).

3.3. Hcy-suppressive nMt-ETC-Com genes identification

We examined the correlation between nMt-ETC-Com gene mRNA levels with Hcy and methylation-related metabolites by linear regression analysis in 6 mouse tissues. We identified 15 nMt-ETC-Com genes whose tissue mRNA levels negatively correlated with Hcy levels (Fig. 2A) and named them as Hcy-suppressive nMt-ETC-Com genes. These 15 Hcy-suppressive nMt-ETC-Com genes include 11 nMt-ETC-Com I genes (NDUFA1/2/3/5, NDUFB2/7, NDUFC1, NDUFS3/7 and NDUFV1/2) one Com IV (COX6C) and two Com V genes (ATP5F1 and ATP5J2). As shown in Fig. 3, these 15 Hcy-suppressive nMt-ETC-Com genes were strongly negatively correlated with tissue Hcy levels (r^2

Table 2
Correlation between nMt-ETC-Com genes (subunits) mRNA levels and Hcy metabolites in mouse tissues.

Gene ID#	Names	Hcy	SAH	SAM	SAM:SAH
Mitochondrial Complex I (45):					
8	NDUF**A1**	-	±	±	±
9	NDUF**A2**	-	±	±	±
10	NDUF**A3**	-	±	±	±
11	NDUF**A4***	-	±	±	±
12	NDUFA5	-	±	±	±
13	NDUFA6	±	±	±	±
14	NDUFA7	±	±	±	±
15	NDUFA8	±	±	±	±
16	NDUFA9	±	±	±	±
17	NDUFA10	±	±	±	±
18	NDUFA11	±	±	±	±
19	NDUFA12	±	±	±	±
20	NDUFA13	±	±	±	±
21	NDUFAB1	±	±	±	±
22	NDUFB1	±	±	±	±
23	NDUF**B2**	-	±	±	±
24	NDUFB3	±	±	±	±
25	NDUFB4	±	±	±	±
26	NDUFB5	±	±	±	±
27	NDUFB6	±	±	±	±
28	NDUF**B7**	-	±	±	±
29	NDUFB8	±	±	±	±
30	NDUFB9	±	±	±	±
31	NDUFB10	±	±	±	±
32	NDUFB11	±	±	±	±
33	NDUF**C1**	-	±	±	±
34	NDUFC2	±	±	±	+
35	NDUFS1	±	±	±	±
36	NDUFS2	±	±	±	±
37	NDUF**S3**	-	±	±	±
38	NDUFS4	±	±	±	±
39	NDUFS5	±	±	±	±
40	NDUFS6	±	±	±	±
41	NDUF**S7**	-	±	±	±
42	NDUFS8	±	±	±	+
43	NDUF**V1**	-	±	±	±
44	NDUF**V2**	-	±	±	±
45	NDUFV3	±	±	±	±
Mitochondrial Complex II (4):					
46	SDHA	±	±	±	±
47	SDHB	±	±	±	±
48	SDHC	±	±	±	±
49	SDHD	±	±	±	±

Gene ID#	Names	Hcy	SAH	SAM	SAM:SAH
Mitochondrial Complex III (10):					
50	CYC1	±	±	±	±
52	UQCR10	±	±	±	±
53	UQCR11	±	±	±	±
54	UQCRB	±	±	±	±
55	UQCRC1	±	±	±	±
56	UQCRC2	±	±	±	±
57	UQCRFS1	±	±	±	±
58	UQCRH	±	±	±	±
59	UQCRQ	±	±	±	±
Mitochondrial Complex IV (19):					
60	COX4I1	±	±	±	±
61	COX4I2	±	±	±	±
62	COX5A	±	±	±	±
63	COX5B	±	±	±	±
64	COX6A1	±	±	-	±
65	COX6A2	±	±	±	±
66	COX6B1	±	±	±	±
67	COX6B2	±	±	±	±
68	COX**6C**	-	±	±	±
69	COX7A1	±	±	±	±
70	COX7A2	±	±	±	±
71	COX7B	±	±	±	±
72	COX7B2	±	±	±	±
73	COX7C	±	±	±	±
74	COX8A	±	±	-	±
75	COX8C	±	±	±	±
Mitochondrial complex V (19):					
79	ATP5A1	±	±	±	±
80	ATP5B	±	±	±	±
81	ATP5C1	±	±	±	±
82	ATP5D	±	±	±	±
83	ATP5E	±	±	±	±
84	ATP5**F1**	-	±	±	±
85	ATP5G1	±	±	±	±
86	ATP5G2	±	±	±	±
87	ATP5G3	±	±	±	±
88	ATP5H	±	±	±	±
90	ATP5J	±	±	±	±
91	ATP5**J2**	-	±	±	±
92	ATP5L	±	±	±	±
93	ATP5L2	±	±	±	±
94	ATP5O	±	±	±	±
95	ATPIF1	±	±	±	±

Table 2. Correlation between nMt-ETC-Com genes (subunits) mRNA levels and Hcy metabolites in mouse tissues. mRNA levels of 84 Mt-ETC-com genes were determined by mining EST databases. The levels of Hcy metabolites were measured by LC-ESI-MS/MS **(Figure 2A)** in six mouse tissues as described in the Methods section. Gene expression levels are expressed as relative expression units (REU), obtained as described in **(Figure 4),** and were plotted against Hcy metabolites levels for correlation analysis. Symbols were used to define the correlation type. "-", negative correlation; "+", positive correlation and "±", no correlation. **Grey background** denotes statistically significant correlation. . ***NDUFA4 was initially included, but is lately not considered as a Com I subunit.**

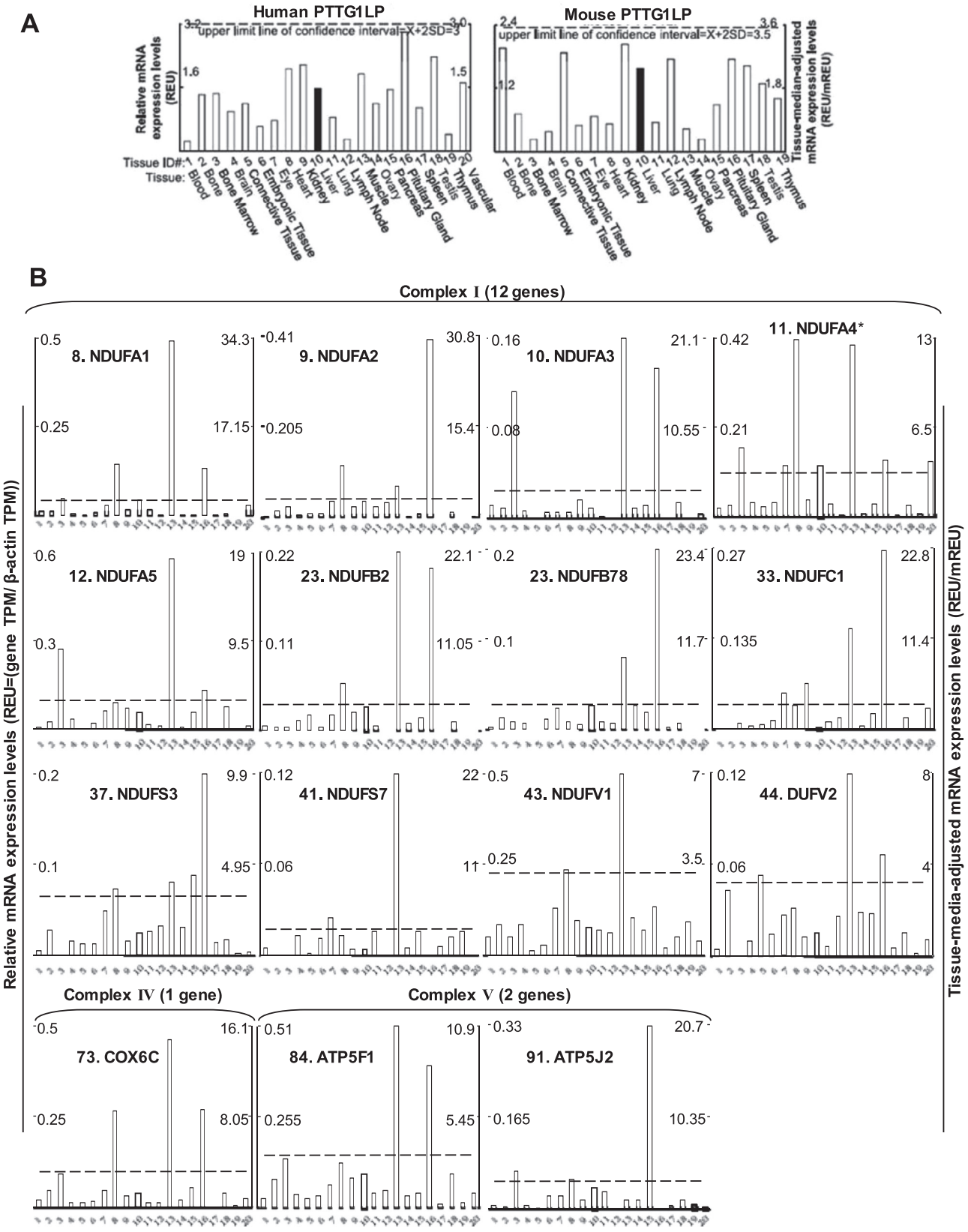

(caption on next page)

Fig. 4. Tissue expression profile of Hcy-suppressive Mt-ETC-Com genes. Twenty human and 19 mouse tissues were given tissue ID numbers and examined for mRNA expression by mining human and mouse EST databases on the NCBI-UniGene site (http://www.ncbi.nlm.nih.gov/unigene). Note that mouse vascular tissue is missing because it is absent in that database. Relative mRNA expression (REU) of the gene is obtained by normalizing gene transcripts per million (TPM) with that of β-actin. Tissue-median-adjusted mRNA expression levels (REU/mREU) were calculated for all genes. A: Confidence interval of 3 housekeeping genes' mRNA expression were established. Dashed lines are upper limits of the confidence intervals of the housekeeping genes. Left and right Y axes describe REU and REU/mREU, respectively. A. Representative tissue mRNA distribution profiles of housekeeping gene TTG1LP in human and mouse. See experimental procedure for more details. B-C. mRNA distribution profiles of Hcy-suppressive Mt-ETC-com genes in 20 human and 19 mouse tissues. The statistical significance was defined when gene expression exceeded the upper limit of the confidence interval. Abbreviations and number in front of the gene names in the graph is consistent with that in (Sup. Table 1). * NDUFA4 was initially included, but lately not consider as Com I subunit.

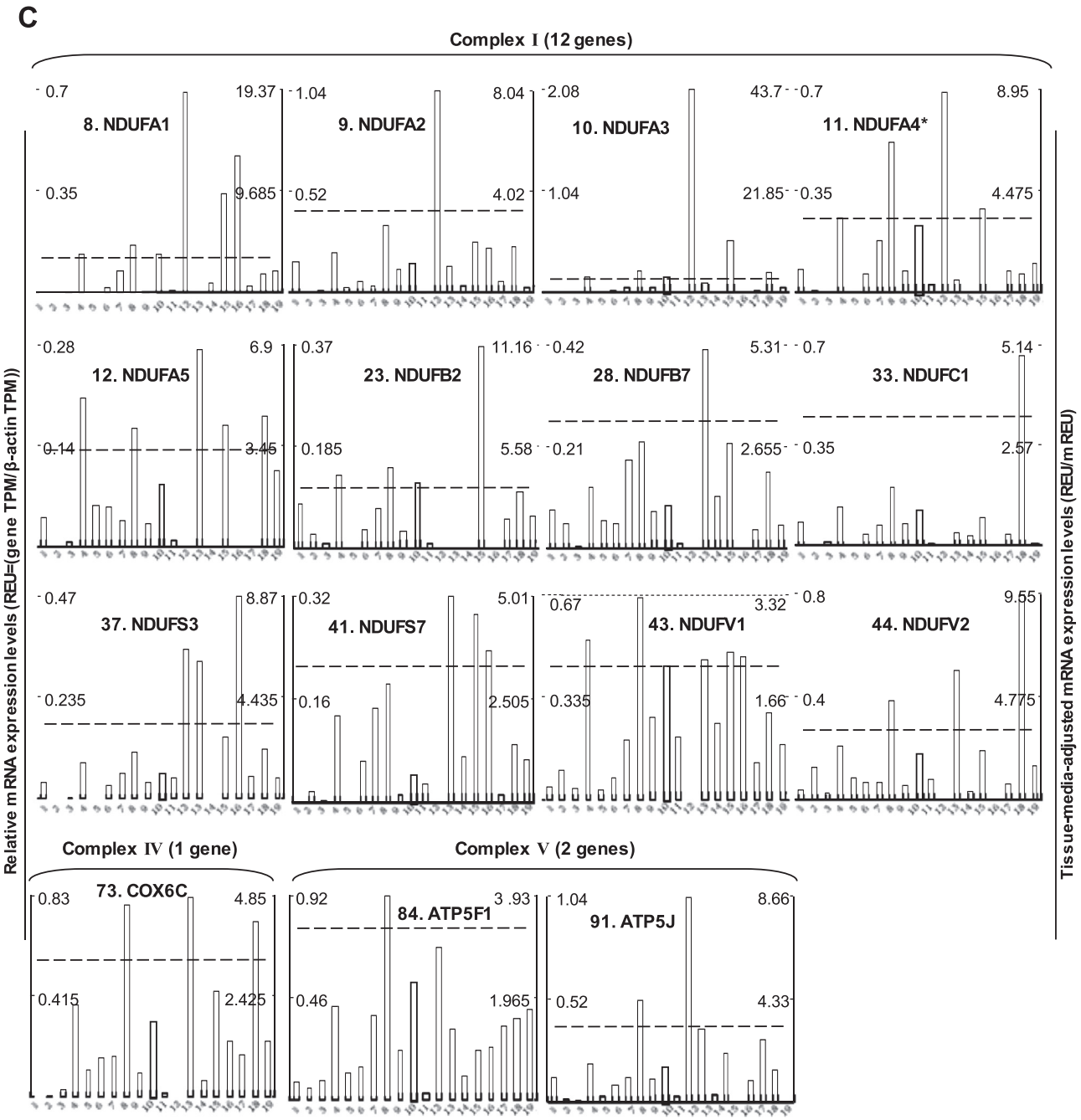

Fig. 4. (*continued*)

ranging from 0.9145 to 0.6578 and p value from 0.0028 to 0.0502).

3.4. Tissue expression profile of Hcy-suppressive nMt-ETC-Com genes

Tissue expression profiles of 15 Hcy-suppressive nMt-ETC-Com genes were established in 20 human and 19 mouse tissues and presented in Fig. 4. All Hcy-suppressive nMt-ETC-Com genes were broadly expressed in human and mouse tissues. In general, these genes have much higher tissue-media-adjusted mRNA expression levels (REU/mREU) in humans than in mice. The REU/mREU indexes were doubled or even greater except that for NDUFA3, NDUFS3 and NDUFV2, which had similar REU/mREU indexes in both species.

In human tissues, the higher scales of REU/mREU were mostly determined by the outstanding REU/mREU index of these genes in muscle and pituitary gland. In human muscle, 14 out of 15 genes were highly expressed (e.g. had high REU/mREU above the upper limit lines of confidence intervals). Human heart had eight genes highly expressed, including NDUFA1/2/4, NDUFB2, NDUFS3, NDUFV1, COX6C, and ATP5J2. In human pituitary gland, 11 genes were highly expressed. Human BM had five genes highly expressed (NDUFA1/3/4/5 and

Table 3
Tissue classification of Hcy-suppressive nMt-ETC-Com genes (subunits) in human and mouse.

A. Human tissue classification

Complex	Com I												Com IV	Com V	
Gene Brief	Supernumerary subunits								Core subunits						
Tissues	A1	A2	A3	A4*	A5	B2	B7	C1	S3	S7	V1	V2	6C	F1	J2
Tier 1. High-Hcy responsive tissues (all Hcy-suppresive nMt ETC complex genes detected)															
Blood	+	+	+	+	+	+	+	+	+	+	+	+	+	+	+
Brain	+	+	+	+	+	+	+	+	+	+	+	+	+	+	+
ET	+	+	+	+	+	+	+	+	+	+	+	+	+	+	+
Eye	+	+	+	++	+	+	+	++	+	++	+	+	+	+	+
Heart	+++	++	+	+++	+	++	+	+	++	+	++	+	++	+	++
Kidney	+	+	+	+	+	+	+	++	+	+	+	+	+	+	+
Liver	+	+	+	++	+	+	+	+	+	+	+	+	+	+	+
Lung	+	+	+	+	+	+	+	+	+	+	+	+	+	+	+
Muscle	+++++	++	++++	+++	+++	++++	++	+++	++	++++	++	++	+++	+++	+
Ovary	+	+	+	+	+	+	+	+	+	+	+	+	+	+	+
Pancreas	+	+	+	+	+	+	+	+	++	+	+	+	+	+	++++
Testis	+	+	+	+	+	+	+	+	+	+	+	+	+	+	+
Tier 2. Mid-Hcy responsive tissues (≤3 Hcy-suppresive nMt ETC complex genes undetected)															
Bone	+	+	+	+	+	+	+	-	+	-	+	+	+	+	+
Bone Marrow	++	+	+++	++	++	+	+	+	-	-	+	-	+	+	++
CT	+	+	-	+	+	+	-	+	+	+	+	++	+	+	+
Pituitary Gland	++	+++++	+++	++	++	++++	++++	++++	++	-	+	++	++	++	-
Vascular	+	+	+	++	+	-	-	+	+	-	+	+	+	+	+
Tier 3. Low-Hcy responsive tissues (≥4 Hcy-suppresive nMt ETC complex genes undetected)															
Lymph Nodes	+	+	-	+	+	-	+	+	+	-	+	+	+	+	-
Spleen	+	-	-	+	-	-	+	-	+	+	+	+	-	+	+
Thymus	-	-	-	+	+	-	-	-	+	+	+	+	+	+	+

B. Mouse tissue classification

Tier 1. High-Hcy responsive tissues (all Hcy-suppresive nMt ETC complex genes detected)																
Brain	++	+	++	++	++	++	+	++	+	+	+	+	+	+	+	+
ET	+	+	+	+	+	+	+	+	+	+	+	+	+	+	+	+
Eye	+	+	+	+	+	+	+	+	+	+	+	+	+	+	+	+
Heart	++	+	++	++	++	++	+	++	+	+	+	++	++	++	++	++
Kidney	+	+	+	+	+	+	+	+	+	+	+	+	+	+	+	+
Liver	++	+	++	+	+	++	+	+	+	+	+	+	+	+	+	+
Pancreas	++	+	+++	++	++	+++	+	+	+	++	+	+	+	+	+	++
Testis	+	+	++	+	++	+	+	+++	+	+	+	++	++	+	+	+
Thymus	+	+	+	+	+	+	+	+	+	+	+	+	+	+	+	+
Tier 2. Mid-Hcy responsive tissues (≤3 Hcy-suppresive nMt ETC complex genes undetected)																
Bone Marrow	+	+	-	-	+	+	+	+	+	+	+	+	+	+	+	+
Lung	+	+	-	+	+	+	+	+	+	+	+	+	+	+	+	+
Muscle	-	+	+	+	++	-	++	+	++	++	+	++	++	+	+	+
Spleen	+	+	+	+	-	+	+	+	+	+	+	+	+	+	+	+
Tier 3. Low-Hcy responsive tissues (≥4 Hcy-suppresive nMt ETC complex genes undetected)																
Blood	-	+	-	+	+	+	+	+	+	-	+	+	-	+	-	
Bone	-	-	-	+	-	+	+	-	-	+	+	+	+	+	-	
CT	-	+	-	-	+	-	+	-	-	-	+	+	+	+	-	
Lymph Nodes	+++	++	++++++	++	-	-	-	-	++	-	-	-	-	+	-	
Ovary	+	+	-	-	-	-	+	+	-	+	+	+	+	+	+	
Pituitary Gland	+++	+	-	-	-	-	-	-	++	++	+	-	+	+	+	

Table 3. Tissue classification of Hcy-suppressive Mt-ETC-com genes (subunits) in human and mouse. Based on tissue expression pattern of Hcy-suppressive Mt-ETC-com genes, human (A) and mouse (B) tissues were classified in tiers and established a tissue Hcy-responsiveness status. Tier 1 tissues expresse all the Hcy-suppressive Mt-ETC-com genes and are named "High-Hcy responsive tissues", tier 2 tissues have 3 or less undetected (very low expression) Hcy-suppressive Mt-ETC-com genes and are named "Mid-Hcy responsive tissues" and tier 3 tissues have 4 or more undetected (very low expression) Hcy-suppressive Mt-ETC-com genes and are named "Low-Hcy responsive tissues". Symbols were used to define mRNA expression levels based on REU/mREU. "-", no expression (REU/mREU 0); "+", (> 0) but less than the upper limit; "++", greater than the upper limit but < 10; "+++", > 10 but < 20; "++++", > 20 but < 30; "+++++", > 30 but < 40 and "++++++", ≥40. *NDUFA4 was initially included, but is lately not considered as a Com I subunit.

ATP5J2).

In contrast, in mouse tissues, REU/mREU peaks were randomly distributed in different tissues, including LN, muscle, testis, PG and pancreas, which determined the scales of the REU/mREU index. In mouse heart, 10 genes were highly expressed, including NDUFA1/3/4/5, NDUFB2, NDUFC1, NDUFV2, COX6C, ATP5F1 and ATP5J2. Mouse pancreas tissue had seven genes highly expressed (NDUFA1/3/4/5, NDUFB2, NDUFS7 and ATP5J2). There were fewer Hcy-suppressive nMt-ETC-Com genes highly expressed in mouse brain (6 genes; NDUFA1/3/4/5, NDUFB2, and NDUFC1), testis (5 genes; NDUFA3/5, NDUFC1, NDUFV2 and COX6C), liver (3 genes; NDUFA1/3, and NDUFB2), lymph node (5 genes; NDUFA1/2/3/4 and NDUFS3) and pituitary gland (3 genes; NDUFA1 and NDUFS3/7).

3.5. Tissue classification of Hcy-suppressive nMt-ETC-Com genes in human and mouse

We classified human and mouse tissues into 3 tiers based on their feature of preferential Hcy-suppressive nMt-ETC-Com gene expression pattern (Table 3). Tier 1 tissue was termed as high-Hcy-responsive tissues with all Hcy-suppressive nMt-ETC-Com genes detected. Tier 2 tissue was termed as mid-Hcy-responsive tissue with three or less undetected (very low expressed) genes. Tier 3 tissue was termed as low-Hcy-responsive tissues with four or more undetected (very low expressed) genes.

Among the Tier 1 tissues (12 in human and 9 in mice), eight tissues shared high-Hcy-responsive features in both human and mice (brain, embryonic tissue, eye, heart, kidney, liver, pancreas and testis). In the remaining four human Tier 1 tissues, blood and ovary were classified as mouse tier 3, whereas lung and muscle as mouse tier 2. The remaining one mouse Tier 1 tissue thymus was classified as human Tier 3. In Tier 2 tissues, we included five human tissues (bone, BM, CT, PG and vascular) and four mouse tissues (BM, lung, muscle and spleen). Only BM shared mid-Hcy-responsive features in both human and mouse. tissues The other three human tier 2 tissues (bone, CT, and PG) were classified as mouse tier 3. Among the remaining three mouse Tier 2 tissues, lung and muscle were classified as human Tier 1 and spleen as human Tier 3. Finally, Tier 3 tissues described three human tissues (LN, spleen and thymus) and six mouse tissues (blood, bone, CT, LN, ovary and PG), with only LN sharing low-Hcy-responsive features in both species.

3.6. Most of the Hcy-suppressive nMt-ETC-Com genes were reduced in experimental hyperhomocysteinemic conditions

We examined the expression of Hcy-suppressive Mt-ETC-com complex genes in 3 HHcy-related gene expression microarrays from the GEO dataset database (GSE9490, GSE56458 and GSE5260) **(**Table 4**).** The GEO is an international public functional genomics data repository that freely distributes microarray, next-generation sequencing, and other forms of high-throughput functional genomics data submitted by the research community. We found that 11 of these genes (NDUFA2/3/5, NDUFB7, NDUFC1, NDUFS3, NDUFV1/2, COX6C, ATP5F1 and ATP5J2) were reduced in Hcy-treated (100 μm, 14 days) human aortic smooth muscle cells (HASMC). Eight genes (NDUFA3/5, NDUFB7, NDUFS3, NDUFV2, COX6C, ATP5F1 and ATP5J2) were decreased in mouse neural retina (MNR) from mice with high methionine (HM, 0.5%) in drinking water for 5 weeks. Two genes (NDUFB7 and NDUFV1) were reduced in dog cardiac cells (DCC) from dogs with methionine (10 g/L) in the drinking water for 2 weeks.

3.7. Hcy-suppressive nMt-ETC-Com genes impact on complex assembly and activity

We searched functional impact of Hcy-suppressive Mt-ETC-com gene on Mt complex assembly and activity in human diseases and experimental models through intensive literature research **(**Table 5**).** Among com I genes, mutations of NDUFA1/2/4, NDUFS3/7 and NDUFV1/2 genes were identified in Leigh syndrome, developmental delay, myoclonic epilepsy, epilepsy, mitochondrial respiratory chain disorder, neurodegenerative disorder, severe muscle complex I enzyme defect, unspecified encephalomyopathy, leukoencephalopathy, bipolar disorder and cardioencephalomyopathy. In the same manner, deficiency of Com I genes (NDUFA1/3/5, NDUFB2/7, NDUFC1, NDUFS3) and Com V gene (ATP5F1) were associated with the inhibition of complex activity/assembly in numerous cell and disease animal models. There was no evidence to connect COX6C (Com IV) and ATP5J2 (Com

Table 4
Hcy-suppressive nMt ETC-Com genes (subunits) expression change (GEO dataset database).

Complex	Model (Tx) GEO ID (ID#.Name)	HASMC (100μM, 14D) GSE9490		MNR (HM, 5 wks) GSE56458		DCC (Met, 2 wks) GSE5260	
		Fold Δ	P-Value	Fold Δ	P-Value	Fold Δ	P-Value
I	8. NDUF**A1**	1.03	0.6401	1.05	0.9415	-1.06	0.8971
	9. NDUF**A2**	**-1.59**	0.0019	-1.01	0.7400	-1.13	0.7121
	10. NDUF**A3**	**-1.29**	0.0271	**-148.84**	0.0014	N/A	N/A
	11. NDUF**A4***	1.21	0.1993	-1.00	0.2071	-1.33	0.4830
	12. NDUF**A5**	**-1.83**	3.16E-05	**-83.59**	0.0014	2.45	0.2896
	23. NDUF**B2**	-1.04	0.6484	1.32	0.1870	-2.26	0.0646
	28. NDUF**B7**	N/A	N/A	**-11.29**	0.0227	**-4.23**	0.0305
	33. NDUF**C1**	**-1.47**	0.0008	-1.12	0.5713	-1.51	0.3570
	37. NDUF**S3**	-1.12	0.2042	**-4.19**	0.0012	-2.46	0.1064
	41. NDUF**S7**	1.03	0.7567	-3.10	0.1856	-1.46	0.2575
	43. NDUF**V1**	**-1.61**	0.0197	-1.24	0.1774	**-2.72**	0.0236
	44. NDUF**V2**	**-1.57**	0.0005	**-117.11**	0.0013	-1.81	0.0775
IV	73. COX**6C**	**-1.71**	0.0005	**-12.77**	0.0023	-1.05	0.8993
V	84. ATP5**F1**	-1.02	0.7635	**-2.73**	0.0028	**-1.27**	0.4980
	91. ATP5**J2**	**-1.82**	0.0005	**-1.05**	0.0527	N/A	N/A

Table 4. Hcy-suppressive nMt ETC complex gene expression change (GEO dataset database). Hcy-suppressive nMt-ETC-Com genes were screened in 3 HHcy-related microarray analyses in the GEO dataset database. * **NDUFA4 was initially included, but is lately not considered as a Com I subunit.**

Table 5
Function of Hcy-suppressive nMt-ETC-Com genes (subunits) on Mt complex assembly/activity.

Com	Genes (ID#. Name)	Disease models (**a:** Human disease, **b**: Experimental models)	Corresponding complex Activity	Corresponding complex Assembly	Reference
I	8. NDUF**A1**	**a:** Leigh S (mu), DD & ME (mu) **a:** MRCD (mu), NDD & SMCED (mu) **b:** Chinese hamster cell (mu), N. Crassa (mu)	↓, ↓ N/A, ↓ ↓, ↓, ↓, ↓, ↓	↓, N/A↓, ↓ ↓, ↓, ↓, ↓, ↓	(57,63-70)
	9. NDUF**A2**	**a:** Leigh S (mu)	↓	↓	(85)
	10. NDUF**A3**	**b:** HEK293 cells (miRNAs KO)	↓	↓	(86)
	11. NDUF**A4***	**a:** Leigh S (mu)	(Com IV↓)	N/A	(84)
	12. NDUF**A5**	**b:** Mouse ELP (partially KO in neuron), Rat IHF (↓ Exp) **b:** HEK293 cells (miRNAs KO)	↓, ↓ ↓	↓, N/A ↓	(58,86,87)
	23. NDUF**B2**	**b:** HEK293 cells (shRNA KO)	↓	NI	82
	28. NDUF**B7**	**b:** HEK293 cells (shRNA KO)	↓	↓	82
	33. NDUF**C1**	**b:** HEK293 cells (shRNA KO)	↓	↓	82
	37. NDUF**S3**	**a:** Leigh S (mu), Unspecified ELMP (mu) **b:** Mouse liver Mt (GzmA treated), HEK293 (shRNA KO)	↓, ↓ ↓, ↓	N/A, N/A N/A, N/A	47-50
	41. NDUF**S7**	**a:** Leigh S (mu), Bipolar disorder (↓ Exp)	↓, ↓, ↓, ↓	↓, ↓, ↓, N/A	(42,51-53)
	43. NDUF**V1**	**a:** Leigh S (mu), LEP and Epilepsi (mu) **b:** Rat IHF (↓ Exp) ,Yeast (mu), C. elegans (mu)	↓, ↓, ↓, ↓, ↓ ↓, ↓, ↓	↓, ↓, N/A, ↓, N/A N/A, ↓, N/A	(42,54-60)
	44. NDUF**V2**	**a:** CELMP (mu), HCM and ELP (mu), Leigh S (mu)	↓, ↓, ↓	N/A, N/A, N/A	(48,61)
IV	73. COX**6C**	N/A	N/A	N/A	N/A
V	84. ATP5**F1**	**b:** Mouse type I diabetic (STZ) interfibrillar heart Mt (↓ Exp)	↓	N/A	(71)
	91. ATP5**J2**	N/A	N/A	N/A	N/A

Table 5. **Function of Hcy-suppressive nMt-ETC-Com genes (subunits) on Mt complex assembly/activity.** The function of studied genes on complex activity and assembly was established through intensive literature research. **"a"** implies disease in human or animal model. **"b"** indicates experimental models used. Words in the parentheses describe the nature of the changes for the indicated gene. Activity/assembly and references corresponding in sequence to a singly study are separated by comma, wherein disease/experimental model may be cited more than once. ***NDUFA4 was initially included, but is lately not considered as a Com I subunit. Abbreviation:** Leigh S, Leigh syndrome; Mu, mutation; DD, developmental delay; ME, myoclonic epilepsy; MRCD, mitochondrial respiratory chain disorder; NDD, neurodegenerative disorder; SMCED, severe muscle complex I enzyme defect; N. Crassa, Neurospora crassa; ELP, encephalopathy; IHF, ischemic heart failure; Exp, expression; ELMP, encephalomyopathy; LEP, leukoencephalopathy; Epil, epilepsy; C. elegans, Caenorhabditis elegans; CELMP, cardioencephalomyopathy; Com, complex; HCM, hypertrophic cardiomyopathy; STZ: streptozotocin; N/A, not analyzed. * **NDUFA4 was initially included, but is lately not considered as a Com I subunit.**

V) with assembly/activity changes.

4. Discussion

In this study, we investigated the effect of HHcy metabolism on nMt-ETC-Com genes by examining mouse tissue Hcy metabolites and gene expression using analytical chemical analysis, database mining, and intensive literature research approaches. We reported the following five major findings: 1) Hcy is differentially metabolized in mouse tissues (differential tissue distribution of metabolites); 2) nMt-ETC-Com genes are differentially expressed in human and mouse tissues; 3) 15 nMt-ETC-Com (11 in Com I) genes are negatively correlated with tissue Hcy levels and defined as Hcy-suppressive genes; 4) human/mouse tissues are classified into 3 tiers for Hcy responsiveness; 5) Hcy-suppressive nMt-ETC-Com genes impact on Mt complex assembly and activity; 6) HHcy may disrupt Mt redox homeostasis mostly via suppressing Mt complex I core subunits NDUFV1/2 and NDUFS3/7 (Fig. 1). We hypothesize that HHcy may cause Mt dysfunction primarily via Hcy-suppressive nMt-ETC-Com I core genes, leading to Mt redox homeostasis disruption.

4.1. Tissue Hcy metabolism

Our study largely revised tissue Hcy metabolic profile. Considering the proposed role of HHcy as an effector for Mt biogenesis, Mt-ETC gene expression and function [21], we investigated the metabolic link between HHcy and nMt-ETC-Com gene expression. Previously, we examined the relationship of Hcy metabolic enzyme expression with the only suitable tissue metabolite dataset to the best of our knowledge, published in 1983 [36] and 1984 [37] using liquid chromatography (LC) [31,32]. In this study, we employed the most sophisticated chemical approach (LC-ESI-MS/MS) and characterized key Hcy metabolites in six mouse tissues **(**Fig. 2**A)**. Compared to previously used LC dataset, our assay detected higher levels of tissue Hcy and SAH **(**Sup. Table 2**)**. For example, in mouse heart tissue, we detected 4.6 nmol/g Hcy and 5.1 nmol/g SAH, whereas the old LC method detected 1.12 nmol/g Hcy and 0.4 nmol/g SAH. In addition, we found a large discrepancy regarding liver tissue, where the old LC method showed that liver Hcy levels were the highest (3.63 nmol/g). In contrast, our result showed that kidney has much higher Hcy levels than liver. Following the same line, the old LC method reported that liver had higher SAM levels. However, we show that lung has the highest SAM levels. We believe LC-ESI-MS/MS is much more sensitive and accurate than the traditional simple LC analysis. Our data indicates that Hcy levels are higher in the lung, kidney and spleen and much lower in the liver. The relative low liver Hcy level may be due to high CBS expression in the liver [31]. Different tissue distribution of Hcy metabolites supports the hypothesis that differential Hcy metabolic enzymes expression attributed to tissue specific Hcy metabolism.

We found that SAH varies greatly between tissues (from 1.6 to 58 nMol/g, up to 36 fold difference) and is the determinant of SAM:SAH ratio, a methylation status indicator [36,37]. Liver has the highest SAH

levels (36 fold that in spleen containing the lowest levels of SAH), which correspond to the lowest SAM:SAH ratio (2% of that in spleen). Our data indicated that spleen, brain, heart, and lung tissues have much higher methylation power and demand. In contrast, liver and kidney have much lower methylation demand, because the SAM:SAH ratio is about 10-fold (or more) higher in spleen, brain, heart and lung than that in liver and kidney.

We previously proposed that HHcy causes CVD via SAH accumulation related hypomethylation [1,38,39]. Our current metabolic study supports the theory that SAH is the metabolic sensor determining methylation status. Interestingly, tissue SAH levels did not always correspond with Hcy levels as we predicted. For example, liver has the highest SAH, but relative low Hcy. In contrast, spleen has the lowest SAH, but very high Hcy. This suggests that SAH synthesis is dominant in the liver, but Hcy synthesis is predominant in the spleen (Fig. 2**C&D**). SAM is relatively consistent and abundant in all tested tissues suggesting that this methyl donor is readily available and may not modulate methylation status determined by SAM:SAH ratio in general. Interestingly, Hcy levels are much lower in heart and brain suggesting Hcy clearance pathways (transsulfuration and/or remethylation) are highly active there to maintain a low threshold. In future studies it would be interesting to investigate tissue-preferred pathways for Hcy metabolism.

It is important to notice that Hcy can be metabolized to become cysteine by the enzymes CBS and CSE (Fig. 2), and generate H_2S, an anti-oxidant. We recently discovered that HHcy suppresses CSE, reduces H_2S and ROS, leading to xx (IKCa) inactivation and impaired EDHF-induced vascular relaxation [38]. Studies in our laboratory are undergoing to investigate the role of HHcy and H_2S on mitochondrial function.

4.2. nMt-ETC-Com genes expression connection to HHcy metabolism and disease

We considered that the expression levels of nMt-ETC-Com genes reflect the overall status of tissue Mt bioenergetics demand. From tissue expression profile analysis **(**Table 1**),** we found that human tissues have higher levels of nMt-ETC-Com gene expression compared to that in mice. Among the identified high energy demanding tissues, heart appears to be consistent in both species and had 57.7% and 58.7% of 78 nMt-ETC-Com genes expressed in human and mice, respectively, suggesting that Mt bioenergetics is essential for heart homeostasis in both species [39]. Most of the tissues displayed very different levels of nMt-ETC-Com gene expression between species. For example, human muscle, pituitary gland and BM have much higher levels of nMt-ETC-Com gene expression than that in mice (84.6%, 67.9% and 19.2 vs 32%, 24% and 0%). In contrast, human lymph node and pancreas have much lower levels of these genes expression (3.8% and 11.5% vs 42.7% and 49.3%). Our data suggested that Mt energy metabolism might play a critical role in endocrine system regulation in pituitary gland. Human BM maybe more dependent on Mt energy supply for hematopoietic cell differentiation than that in mice. Lower Mt gene expression in mouse muscle may be related with limited muscle activity in mice. The robust expression of nMt-ETC-Com gene in mouse LN, but not in human is likely due to high demand of the immune response to identify and fight infection, a major function of LN, since mice are often exposed to a hostile pathogen environment. Mouse pancreas tissue presented high Mt energy demand, which may be related with high digestive activity resulting from excessive feeding and limited physical activity. The nMt-ETC-Com gene tissue expression profiles established in this report utilized the expression sequence tag (EST) database, which is a more accurate approach for mRNA evaluation than traditional methods [30,32]. Even without activity validation, this study provided important molecular evidence for species specific gene tissue expression profile and Mt energy homeostasis regulation.

Based on their negative correlation with tissue Hcy levels, we identify 15 Hcy-suppressive Mt-ETC-Com genes **(**Table 2 **&** Fig. 3**),** 11 which are components of Mt-Com I. Mt-Com I is the largest Mt-Com, which contains 44 subunits (Sup. Table 1**)**. Fourteen of 44 Mt-Com I subunits are defined as core subunits as which can accomplish full catalytic function of Mt-Com I [40–45]. Four of the Hcy-suppressive Mt-ETC-Com genes are Com I core subunits (NDUFS3/7 and NDUFV1/2) which are indispensable for complex I activity (NADH oxidation and electron transfer to ubiquinone) and/or assembly/stability [42,46–62]. Among the remaining eight Hcy-suppressive Mt-ETC-Com I genes, (NDUFA1, NDUFA2/3/5, NDUFB2/7and NDUFC1) are all recognized to regulate Com assembly/stability/activity [57,63–70], and NDUFA4 was linked with complex IV activity. These findings led us to hypothesize that HHcy causes Mt dysfunction primarily via Hcy-suppressive Mt-ETC-Com I genes. Our data also suggested that HHcy might suppresses Com IV and V via COX6C, ATP5J2 and ATP5F1 gene inhibitions [71].

We defined 12 human and 9 mouse tissues as high Hcy-responsive tissues **(Tier 1,** Table 3**)** because all 15 Hcy-suppressive nMt-ETC-Com genes were expressed/detected in these tissues. Human tier 1 tissues include endocrine system (pancreas, ovary and testis), lung and muscle, which are affected in Mt-related disease [72,73]. These tissue are likely prone to HHcy-induced defect mostly via Mt-ETC-Com I dysfunction. Among the 8 tier 1 tissues that are overlapped in both species, brain, heart, liver and kidney are recognized in both HHcy-related and Mt-related disease [3,4,8,20,72,74–77]. We recently reported that Hcy-mediated inflammatory monocyte differentiation in human chronic kidney disease (CKD) [78], which provided indirect evidence for Hcy-related kidney injury potentially involving Mt dysfunction. Tier 2 Mid Hcy-responsive tissues lack of up to 3 Hcy-suppressive nMt-ETC-Com gene expression may imply a less sensitive feature to HHcy-induced Mt dysfunction in human bone, BM, connective tissue, pituitary gland, and vasculature. We previously reported that HHcy reduces BM progenitor cells (CD34+/VEGR2+) generation and mobilization leading to blunt re-endothelialization and vascular remodeling [79]. It is possible that HHcy-induced BM effects will not be mediated by Mt dysfunction. Human tier 3 low Hcy-responsive tissues are mostly immune organs (lymph nodes, spleen and thymus) which lack of four or more Hcy-suppresive nMt-ETC-Com genes. Our findings suggest that Mt dysfunction may be an important mechanism for HHcy-induced organ damage in brain, heat, liver and kidney, but not in HHcy-induced immune cell response.

Interestingly, we found that 11 of the 15 Hcy-suppressive nMt-ETC-Com genes identified in this study are down regulated in HHcy experimental models (Table 4). These findings strongly consolidate our correlation analysis results and strengthen the hypothesis that HHcy causes Mt dysfunction via Hcy-suppressive nMt-ETC-Com genes.

4.3. Gene impact on Mt redox homeostasis and potential underlying mechanisms

We established the connection between Hcy-suppressive nMt-ETC-Com genes with Mt redox homeostasis by incorporating our findings with information from single-particle cryo-electron microscopy (cryo-EM) structure analysis [35], and presented a Com I 3D sphere structure model in Fig. 5. Mt-ETC-Com I is the largest complex and has a L shape that consist of 3 modules (N, Q & P modules) [40,41,52,65]. N and Q modules are located in the Mt matrix and responsible for transfer of electrons. The P module is embedded in the Mt inner membrane and pumps protons into the Mt intermembrane space contributing to the proton gradient.

Electrons from the oxidation of NADH are transferred via Flavin mononucleotide (FMN) and a series of iron-sulfur (Fe-S) clusters to Co-Q in the Q module (Fig. 5). The Fe–S clusters are conservative and versatile cofactors required to sustain fundamental life processes, including electron transfer, substrate binding/activation, regulation of gene expression and enzyme activity [80,81]. We identified 11 Hcy-suppressive nMt-ETC-Com I genes. Three of them are located in the N

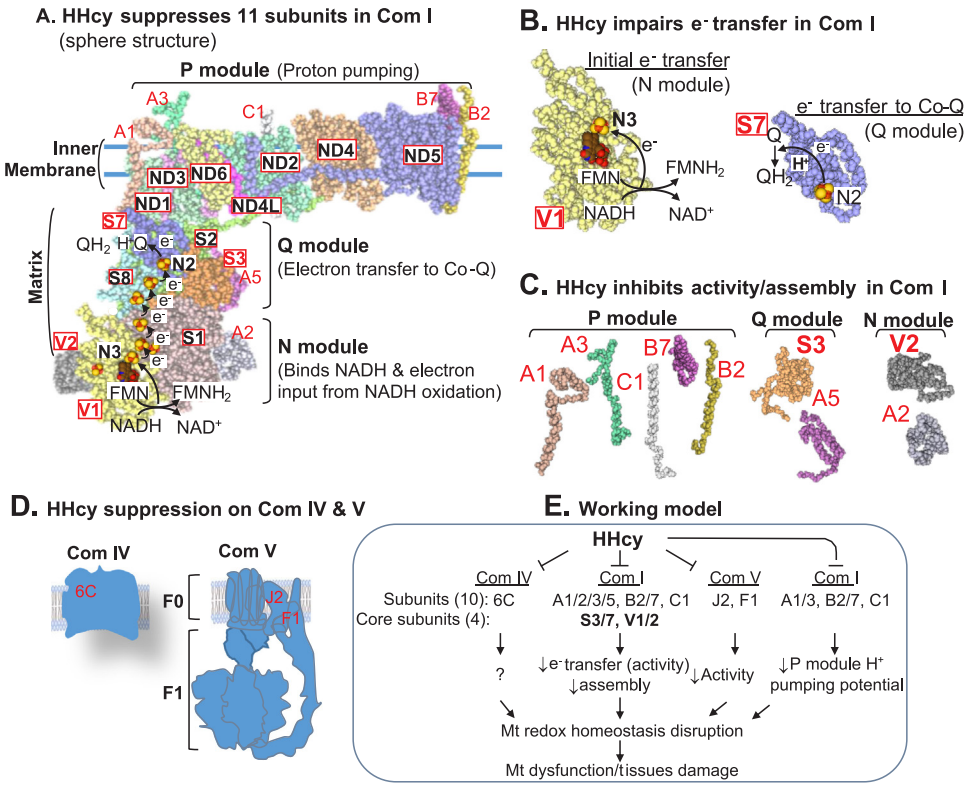

Fig. 5. Functional impact of HHcy on Mt-ETC-Com. The model of HHCY inhibition in MT-ETC-Complexes is established based on Hcy-suppresive nMt-ETC-Com genes identified in Table 3 and information from single-particle cryo-electron microscopy (cryo-EM) structure analysis. **A. HHcy suppresses 11 subunits in Com I (sphere structure).** Com I has an L shaped 3D structure and is divided into 3 modules (N, Q & P). Among the identified 11 Hcy-suppressive nMt-ETC-Com I genes, 4 are core subunits and 7 are supernumerary subunits. Com I electron transfer is initiated from NADH oxidation by Flavin mononucleotide (FMN) to donate 2 electrons, which are then transferred to Co-Q via iron-sulfur (Fe-S) clusters e^- pathway. HHcy suppresses 11 subunits in complex I and impairs Com I functions. **B. HHcy impairs e^- transfer in Com I.** In the N module, HHcy inhibits core subunit V1 and disrupts initial electron transfer from NADH oxidation by FMN or e^- from FMN to the N3 Fe-S cluster. HHcy inhibits core subunit S7 and disrupts e^- transfer to Co-Q. **C. HHcy inhibits activity/assembly in Com I.** HHcy may inhibit Com I activity/assembly via suppression of 5 subunits in the P module, 2 subunits in the Q module and 2 in the N module, which have implicated roles in activity/assembly in Table 6. **D. HHcy suppression on Com IV & V.** HHcy suppresses 3 subunits in Com IV & V. **E. Working model.** HHcy may cause Mt dysfunction and tissue damage mostly via nMt-ETC-Com I genes suppression, especially core subunits S3/7 and V1/2, which leads to impaired e^- transfer/assembly and Mt redox homeostasis dysregulation. HHcy may also impact Com IV/V activity via gene suppression. Mt Com subunits are briefed as A1 (NDUFA1), A2 (NDUFA2), A3 (NDUFA3), A5 (NDUFA5), B2 (NDUFB2), B7 (NDUFB7), S3 (NDUFS3), S7 (NDUFS7), V1 (NDUFV1), V2 (NDUFV2), C1 (NDUFC1), C6 (COX6C), F1 (ATP5F1), and J2 (ATP5J2). Hcy-suppresive nMt-ETC-Com genes are highlighted in red. Core subunits are framed. Fe-Sulfur clusters are modeled as yellow/red spheres (only N3 and N2 are labeled). FMN is modeled as a brown/red sphere complex.

module (V1, V2 and A2), three (S3, S7 and A5) in the Q module, and five in the P module (A1/3, B2/7 and C1) [45,82]. Hcy-suppressive nMt-ETC-Com gene V1 is co-localized with FMN and Fe-S cluster N3 [45,82] and participates in initial electron transfer. V1 mutation is connected with N3 related redox homeostasis disruption [83]. Hcy-suppressive nMt-ETC-Com gene S7 is co-localized with Fe-S cluster N2 and facilitates the final electron transfer to Co-Q [45,82]. Taken together, our findings support the hypothesis that Hcy suppression on nMt-ETC-Com I genes, especially on V1 and S7, may lead to the impairment of the electron transfer cascade, disruption of redox homeostasis and increase in Mt ROS production.

4.4. Gene impact on Mt Com assembling and activity

The five Mt-ETC Com are assembled with 97 proteins in a highly organized pattern to carry out the function of ATP generation through oxidative phosphorylation. Our current studies support the hypothesis that HHcy impairs Mt-ETC Com assembly and activity by suppressing Mt-ETC Com gene expression. This notion is supported by strong evidence from the literature showing that mutation or loss-of-function of 12 of the 15 Hcy-suppressive nMt-ETC-Com genes are implicated in disease and associated with reduced activity and assembly for their corresponding complexes (Table 5). However, mutation of NDUFA4, a Com I subunit, is associated with reduced activity of Com IV activity in Leigh syndrome [84]. We noticed that core subunits S3/7 & V1/2 mutations are characterized in human disease, emphasizing their significant role in human pathophysiology. The nMt-ETC Com supernumerary subunits are usually wrapping around the core subunits, especially in the P module to protect them from oxidation [41,82]. We therefore anticipate that HHcy reduces proton pumping potential by suppressing A1/3, B2/7 and C1 expression and making the P module vulnerable to oxidative insults (Fig. 5**C**). In addition, we also identified three Hcy-suppressive nMt-ETC-Com genes in complexes IV & V (Fig. 5**D**). Even though function analysis information is limited, their function in electron flow, proton pumping and ATP generation may also be influenced by HHcy.

Our current study involved dynamic approaches including 1) database mining on multiple large NCBI databases (experimentally verified human and mouse EST UniGene, GEO dataset and Structure bank), 2) measuring tissue metabolites using most sophisticated technology (LC-ESI-MS/MS), 3) addressing Hcy-suppressive gene function using reported findings in experimental model and human disease (GEO dataset database and literature), and 4) modelling HHcy inhibition on Mt-ETC-Com (NCBI Structure bank). The strategy to combine all these sophisticated approaches is novel and powerful, which allows us to establish systemic hypothesis and potentially impact the research field.

In conclusion, we proposed a hypothetic working model that HHcy causes Mt dysfunction and tissue damage mostly via nMt-ETC-Com I core subunits S3/7 and V1/2 suppression, which leads to impaired e^- transfer, complex assembly and Mt redox homeostasis dysregulation (Fig. 5**E**). Further research in our laboratory is ongoing to validate the expression of the identified 15 Hcy-suppressive genes, their regulatory mechanism and functional implication in different disease models of HHcy. This line of investigation should lead to the identification of therapeutic targets for HHcy-related metabolic and cardiovascular diseases.

Acknowledgments

None.

Funding

This work was supported in part by National Institutes of Health

(NIH) Grants HL67033, HL77288, HL82774, HL-110764, HL130233, HL131460, DK104114 and DK113775 (HW); HL9445, HL108910 and HL116917 (XFY), and by National Natural Science Foundation of China Grants number 81330004 and 91639204 (YJ).

Conflict of interest

The authors declare no financial interests.

Appendix A. Supplementary material

Supplementary data associated with this article can be found in the online version at http://dx.doi.org/10.1016/j.redox.2018.03.015.

References

[1] M.E. Lee, H. Wang, Trends Cardiovasc. Med. 9 (1999) 49–54.
[2] Y. Huo, J. Li, X. Qin, Y. Huang, X. Wang, R.F. Gottesman, G. Tang, B. Wang, D. Chen, M. He, J. Fu, Y. Cai, X. Shi, Y. Zhang, Y. Cui, N. Sun, X. Li, X. Cheng, J. Wang, X. Yang, T. Yang, C. Xiao, G. Zhao, Q. Dong, D. Zhu, J. Ge, L. Zhao, D. Hu, L. Liu, F.F. Hou, JAMA 313 (2015) 1325–1335.
[3] B.A. Maron, J. Loscalzo, Annu. Rev. Med. 60 (2009) 39–54.
[4] R. Obeid, W. Herrmann, FEBS Lett. 580 (2006) 2994–3005.
[5] Z. Cheng, X. Jiang, M. Pansuria, P. Fang, J. Mai, K. Mallilankaraman, R.K. Gandhirajan, S. Eguchi, R. Scalia, M. Madesh, X. Yang, H. Wang, Diabetes 64 (2015) 947–959.
[6] P. Fang, D. Zhang, Z. Cheng, C. Yan, X. Jiang, W.D. Kruger, S. Meng, E. Arning, T. Bottiglieri, E.T. Choi, Y. Han, X.F. Yang, H. Wang, Diabetes 63 (2014) 4275–4290.
[7] D. Xie, Y. Yuan, J. Guo, S. Yang, X. Xu, Q. Wang, Y. Li, X. Qin, G. Tang, Y. Huo, G. Deng, S. Wu, B. Wang, Q. Zhang, X. Wang, P. Fang, H. Wang, F. Hou, Sci. Rep. 5 (2015) 16268.
[8] M. Gulsen, Z. Yesilova, S. Bagci, A. Uygun, A. Ozcan, C.N. Ercin, A. Erdil, S.Y. Sanisoglu, E. Cakir, Y. Ates, M.K. Erbil, N. Karaeren, K. Dagalp, J. Gastroenterol. Hepatol. 20 (2005) 1448–1455.
[9] M.D. Jamaluddin, I. Chen, F. Yang, X. Jiang, M. Jan, X. Liu, A.I. Schafer, W. Durante, X. Yang, H. Wang, Blood 110 (2007) 3648–3655.
[10] H. Wang, X. Jiang, F. Yang, G.B. Chapman, W. Durante, N.E. Sibinga, A.I. Schafer, Blood 99 (2002) 939–945.
[11] D. Zhang, P. Fang, X. Jiang, J. Nelson, J.K. Moore, W.D. Kruger, R.M. Berretta, S.R. Houser, X. Yang, H. Wang, Circ. Res. 111 (2012) 37–49.
[12] D. Zhang, X. Jiang, P. Fang, Y. Yan, J. Song, S. Gupta, A.I. Schafer, W. Durante, W.D. Kruger, X. Yang, H. Wang, Circulation 120 (2009) 1893–1902.
[13] H. Wang, X. Jiang, F. Yang, J.W. Gaubatz, L. Ma, M.J. Magera, X. Yang, P.B. Berger, W. Durante, H.J. Pownall, A.I. Schafer, Blood 101 (2003) 3901–3907.
[14] D. Liao, H. Tan, R. Hui, Z. Li, X. Jiang, J. Gaubatz, F. Yang, W. Durante, L. Chan, A.I. Schafer, H.J. Pownall, X. Yang, H. Wang, Circ. Res. 99 (2006) 598–606.
[15] K. Ma, S. Lv, B. Liu, Z. Liu, Y. Luo, W. Kong, Q. Xu, J. Feng, X. Wang, Cardiovasc. Res. 97 (2013) 349–359.
[16] J. Feng, Z. Zhang, W. Kong, B. Liu, Q. Xu, X. Wang, Cardiovasc. Res. 84 (2009) 155–163.
[17] M.A. Hofmann, E. Lalla, Y. Lu, M.R. Gleason, B.M. Wolf, N. Tanji, L.J. Ferran Jr., B. Kohl, V. Rao, W. Kisiel, D.M. Stern, A.M. Schmidt, J. Clin. Investig. 107 (2001) 675–683.
[18] S. Lim, M.S. Kim, K.S. Park, J.H. Lee, G.H. An, M.J. Yim, J. Song, Y.K. Pak, H.K. Lee, Atherosclerosis 158 (2001) 399–405.
[19] P.S. Ganapathy, R.L. Perry, A. Tawfik, R.M. Smith, E. Perry, P. Roon, B.R. Bozard, Y. Ha, S.B. Smith, Invest. Ophthalmol. Vis. Sci. 52 (2011) 5551–5558.
[20] Y.F. Chou, C.C. Yu, R.F. Huang, J. Nutr. 137 (2007) 2036–2042.
[21] L. Chang, B. Geng, F. Yu, J. Zhao, H. Jiang, J. Du, C. Tang, Amino Acids 34 (2008) 573–585.
[22] J.M. Kim, H. Lee, N. Chang, J. Nutr. 132 (2002) 3418–3421.
[23] K. Perez-de-Arce, R. Foncea, F. Leighton, Biochem. Biophys. Res. Commun. 338 (2005) 1103–1109.
[24] R.C. Austin, S.K. Sood, A.M. Dorward, G. Singh, S.G. Shaughnessy, S. Pamidi, P.A. Outinen, J.I. Weitz, J. Biol. Chem. 273 (1998) 30808–30817.
[25] A. Kumar, L. John, S. Maity, M. Manchanda, A. Sharma, N. Saini, K. Chakraborty, S. Sengupta, J. Biol. Chem. 286 (2011) 21779–21795.
[26] K.M. Holmstrom, T. Finkel, Nat. Rev. Mol. Cell Biol. 15 (2014) 411–421.
[27] X. Li, P. Fang, J. Mai, E.T. Choi, H. Wang, X.F. Yang, J. Hematol. Oncol. 6 (2013) 19.
[28] J. Nunnari, A. Suomalainen, Cell 148 (2012) 1145–1159.
[29] Umdf.org. What is Mitochondrial Disease-The United Mitochondrial Disease Foundation.
[30] Y. Yin, Y. Yan, X. Jiang, J. Mai, N.C. Chen, H. Wang, X.F. Yang, Int. J. Immunopathol. Pharmacol. 22 (2009) 311–322.
[31] N.C. Chen, F. Yang, L.M. Capecci, Z. Gu, A.I. Schafer, W. Durante, X.F. Yang, H. Wang, FASEB J. Off. Publ. Fed. Am. Soc. Exp. Biol. 24 (2010) 2804–2817.
[32] X. Li, J. Mai, A. Virtue, Y. Yin, R. Gong, X. Sha, S. Gutchigian, A. Frisch, I. Hodge, X. Jiang, H. Wang, X.F. Yang, PLOS One 7 (2012) e33628.
[33] X. Huang, R. Gong, X. Li, A. Virtue, F. Yang, I.H. Yang, A.H. Tran, X.F. Yang, H. Wang, J. Biol. Chem. 288 (2013) 15628–15640.
[34] T. Barrett, S.E. Wilhite, P. Ledoux, C. Evangelista, I.F. Kim, M. Tomashevsky, K.A. Marshall, K.H. Phillippy, P.M. Sherman, M. Holko, A. Yefanov, H. Lee, N. Zhang, C.L. Robertson, N. Serova, S. Davis, A. Soboleva, Nucleic Acids Res. 41 (2013) D991–D995.
[35] J. Zhu, K.R. Vinothkumar, J. Hirst, Nature 536 (2016) 354–358.
[36] S. Helland, P.M. Ueland, Cancer Res. 43 (1983) 4142–4147.
[37] P.M. Ueland, S. Helland, O.J. Broch, J.S. Schanche, J. Biol. Chem. 259 (1984) 2360–2364.
[38] Z. Cheng, X. Shen, X. Jiang, H. Shan, M. Cimini, P. Fang, Y. Ji, J.Y. Park, K. Drosatos, X. Yang, C.G. Kevil, R. Kishore, H. Wang, Redox Biol. (2018).
[39] T. Nagoshi, M. Yoshimura, G.M. Rosano, G.D. Lopaschuk, S. Mochizuki, Curr. Pharm. Des. 17 (2011) 3846–3853.
[40] R.S. Vartak, M.K. Semwal, Y. Bai, J. Bioenerg. Biomembr. 46 (2014) 323–328.
[41] K.R. Vinothkumar, J. Zhu, J. Hirst, Nature 515 (2014) 80–84.
[42] G. Leman, N. Gueguen, V. Desquiret-Dumas, M.S. Kane, C. Wettervald, S. Chupin, A. Chevrollier, A.S. Lebre, J.P. Bonnefont, M. Barth, P. Amati-Bonneau, C. Verny, D. Henrion, D. Bonneau, P. Reynier, V. Procaccio, Int. J. Biochem. Cell Biol. 65 (2015) 91–103.
[43] B. Andrews, J. Carroll, S. Ding, I.M. Fearnley, J.E. Walker, Proc. Natl. Acad. Sci. USA 110 (2013) 18934–18939.
[44] M. McKenzie, M.T. Ryan, IUBMB life 62 (2010) 497–502.
[45] M. Lazarou, D.R. Thorburn, M.T. Ryan, M. McKenzie, Biochim. Et. Biophys. Acta 1793 (2009) 78–88.
[46] M. Mimaki, X. Wang, M. McKenzie, D.R. Thorburn, M.T. Ryan, Biochim. Et. Biophys. Acta 1817 (2012) 851–862.
[47] P. Benit, A. Slama, F. Cartault, I. Giurgea, D. Chretien, S. Lebon, C. Marsac, A. Munnich, A. Rotig, P. Rustin, J. Med. Genet. 41 (2004) 14–17.
[48] H. Pagniez-Mammeri, A. Lombes, M. Brivet, H. Ogier-de Baulny, P. Landrieu, A. Legrand, A. Slama, Mol. Genet. Metab. 96 (2009) 196–200.
[49] D. Martinvalet, D.M. Dykxhoorn, R. Ferrini, J. Lieberman, Cell 133 (2008) 681–692.
[50] S. Suhane, H. Kanzaki, V. Arumugaswami, R. Murali, V.K. Ramanujan, Biol. Open 2 (2013) 295–305.
[51] R.H. Triepels, L.P. van den Heuvel, J.L. Loeffen, C.A. Buskens, R.J. Smeets, M.E. Rubio Gozalbo, S.M. Budde, E.C. Mariman, F.A. Wijburg, P.G. Barth, J.M. Trijbels, J.A. Smeitink, Ann. Neurol. 45 (1999) 787–790.
[52] S. Lebon, L. Minai, D. Chretien, J. Corcos, V. Serre, N. Kadhom, J. Steffann, J.Y. Pauchard, A. Munnich, J.P. Bonnefont, A. Rotig, Mol. Genet. Metab. 92 (2007) 104–108.
[53] A.C. Andreazza, L. Shao, J.F. Wang, L.T. Young, Arch. General. Psychiatry 67 (2010) 360–368.
[54] I. Ogilvie, N.G. Kennaway, E.A. Shoubridge, J. Clin. Investig. 115 (2005) 2784–2792.
[55] P. Benit, D. Chretien, N. Kadhom, P. de Lonlay-Debeney, V. Cormier-Daire, A. Cabral, S. Peudenier, P. Rustin, A. Munnich, A. Rotig, Am. J. Human. Genet. 68 (2001) 1344–1352.
[56] C. Vilain, C. Rens, A. Aeby, D. Baleriaux, P. Van Bogaert, G. Remiche, J. Smet, R. Van Coster, M. Abramowicz, I. Pirson, Clin. Genet. 82 (2012) 264–270.
[57] M. Moran, H. Rivera, M. Sanchez-Arago, A. Blazquez, B. Merinero, C. Ugalde, J. Arenas, J.M. Cuezva, M.A. Martin, Biochim. Et. Biophys. Acta 1802 (2010) 443–453.
[58] T. Liu, L. Chen, E. Kim, D. Tran, B.S. Phinney, A.A. Knowlton, Life Sci. 101 (2014) 27–36.
[59] F. Varghese, E. Atcheson, H.R. Bridges, J. Hirst, Human. Mol. Genet. 24 (2015) 6350–6360.
[60] L.I. Grad, B.D. Lemire, Human. Mol. Genet. 13 (2004) 303–314.
[61] P. Benit, R. Beugnot, D. Chretien, I. Giurgea, P. De Lonlay-Debeney, J.P. Issartel, M. Corral-Debrinski, S. Kerscher, P. Rustin, A. Rotig, A. Munnich, Human. Mutat. 21 (2003) 582–586.
[62] J.M. Cameron, N. MacKay, A. Feigenbaum, M. Tarnopolsky, S. Blaser, B.H. Robinson, A. Schulze,) Eur. J. Paediatr. Neurol.: EJPN: Off. J. Eur. Paediatr. Neurol. Soc. 19 (2015) 525–532.
[63] D. Fernandez-Moreira, C. Ugalde, R. Smeets, R.J. Rodenburg, E. Lopez-Laso, M.L. Ruiz-Falco, P. Briones, M.A. Martin, J.A. Smeitink, J. Arenas, Ann. Neurol. 61 (2007) 73–83.
[64] N. Uehara, M. Mori, Y. Tokuzawa, Y. Mizuno, S. Tamaru, M. Kohda, Y. Moriyama, Y. Nakachi, N. Matoba, T. Sakai, T. Yamazaki, H. Harashima, K. Murayama, K. Hattori, J. Hayashi, T. Yamagata, Y. Fujita, M. Ito, M. Tanaka, K. Nibu, A. Ohtake, Y. Okazaki, Ann. Clin. Transl. Neurol. 1 (2014) 361–369.
[65] P. Potluri, A. Davila, E. Ruiz-Pesini, D. Mishmar, S. O'Hearn, S. Hancock, M. Simon, I.E. Scheffler, D.C. Wallace, V. Procaccio, Mol. Genet. Metab. 96 (2009) 189–195.
[66] H.C. Au, B.B. Seo, A. Matsuno-Yagi, T. Yagi, I.E. Scheffler, Proc. Nat. Acad. Sci. USA 96 (1999) 4354–4359.
[67] N. Yadava, P. Potluri, E.N. Smith, A. Bisevac, I.E. Scheffler, J. Biol. Chem. 277 (2002) 21221–21230.
[68] N. Yadava, P. Potluri, I.E. Scheffler, Int. J. Biochem. Cell Biol. 40 (2008) 447–460.
[69] N. Yadava, T. Houchens, P. Potluri, I.E. Scheffler, J. Biol. Chem. 279 (2004) 12406–12413.
[70] I. Marques, M. Duarte, A. Videira, J. Mol. Biol. 329 (2003) 283–290.
[71] T.L. Croston, D.L. Shepherd, D. Thapa, C.E. Nichols, S.E. Lewis, E.R. Dabkowski, R. Jagannathan, W.A. Baseler, J.M. Hollander, Life Sci. 93 (2013) 313–322.
[72] L. Jia, J. Li, B. He, Y. Jia, Y. Niu, C. Wang, R. Zhao, Sci. Rep. 6 (2016) 19436.
[73] J. Chow, J. Rahman, J.C. Achermann, M.T. Dattani, S. Rahman, Nat. Rev. Endocrinol. 13 (2017) 92–104.
[74] S.A. Polyzos, J. Kountouras, K. Patsiaoura, E. Katsiki, E. Zafeiriadou, G. Deretzi, C. Zavos, E. Gavalas, P. Katsinelos, V. Mane, A. Slavakis, Ann. Hepatol. 11 (2012)

68–76.
[75] V. Medici, J.M. Peerson, S.P. Stabler, S.W. French, J.F. Gregory 3rd, M.C. Virata, A. Albanese, C.L. Bowlus, S. Devaraj, E.A. Panacek, N. Rahim, J.R. Richards, L. Rossaro, C.H. Halsted, J. Hepatol. 53 (2010) 551–557.
[76] E.R. Garcia-Tevijano, C. Berasain, J.A. Rodriguez, F.J. Corrales, R. Arias, A. Martin-Duce, J. Caballeria, J.M. Mato, M.A. Avila, Hypertension 38 (2001) 1217–1221.
[77] I.I. Kruman, C. Culmsee, S.L. Chan, Y. Kruman, Z. Guo, L. Penix, M.P. Mattson, J. Neurosci. Off. J. Soc. Neurosci. 20 (2000) 6920–6926.
[78] J. Yang, P. Fang, D. Yu, L. Zhang, D. Zhang, X. Jiang, W.Y. Yang, T. Bottiglieri, S.P. Kunapuli, J. Yu, E.T. Choi, Y. Ji, X. Yang, H. Wang, Circ. Res. 119 (2016) 1226–1241.
[79] J. Nelson, Y. Wu, X. Jiang, R. Berretta, S. Houser, E. Choi, J. Wang, J. Huang, X. Yang, H. Wang, FASEB J.: Off. Publ. Fed. Am. Soc. Exp. Biol. 29 (2015) 3085–3099.
[80] D.C. Johnson, D.R. Dean, A.D. Smith, M.K. Johnson, Annu. Rev. Biochem. 74 (2005) 247–281.
[81] R. Lill, Nature 460 (2009) 831–838.
[82] D.A. Stroud, E.E. Surgenor, L.E. Formosa, B. Reljic, A.E. Frazier, M.G. Dibley, L.D. Osellame, T. Stait, T.H. Beilharz, D.R. Thorburn, A. Salim, M.T. Ryan, Nature 538 (2016) 123–126.
[83] E. Nakamaru-Ogiso (L. Sazanov, Springer, Dordrecht, 2012, 61–79.
[84] R.D. Pitceathly, S. Rahman, Y. Wedatilake, J.M. Polke, S. Cirak, A.R. Foley, A. Sailer, M.E. Hurles, J. Stalker, I. Hargreaves, C.E. Woodward, M.G. Sweeney, F. Muntoni, H. Houlden, J.W. Taanman, M.G. Hanna, U.K. Consortium, Cell Rep. 3 (2013) 1795–1805.